nature aging

ARTICLES

https://doi.org/10.1038/s43587-021-00039-1

Olfactory perception of food abundance regulates dietary restriction-mediated longevity via a brain-to-gut signal

Bi Zhang[1,2,3], Heejin Jun[2,3], Jun Wu[2,3], Jianfeng Liu[1]✉ and X. Z. Shawn Xu[2,3]✉

The role of food nutrients in mediating the positive effect of dietary restriction (DR) on longevity has been extensively characterized, but how non-nutrient food components regulate lifespan is not well understood. Here, we show that food-associated odors shorten the lifespan of *Caenorhabditis elegans* under DR but not those fed ad libitum, revealing a specific effect of food odors on DR-mediated longevity. Food odors act on a neural circuit comprising the sensory neurons ADF and CEP, and the interneuron RIC. This olfactory circuit signals the gut to suppress DR-mediated longevity via octopamine, the mammalian homolog of norepinephrine, by regulating the energy sensor AMP-activated protein kinase (AMPK) through a Gq-phospholipase Cβ-CaMKK-dependent mechanism. In mouse primary cells, we find that norepinephrine signaling regulates AMPK through a similar mechanism. Our results identify a brain–gut axis that regulates DR-mediated longevity by relaying olfactory information about food abundance from the brain to the gut.

Food is a primary environmental factor that affects aging[1,2]. DR represents one of the most effective interventions to extend lifespan in all tested organisms, ranging from yeast to mammals[1,2]. Previous efforts have mostly focused on investigating how nutrients in food affect aging. This has led to the identification of several nutrient signaling pathways, particularly AMP-activated protein kinase (AMPK) and mechanistic target of rapamycin (mTOR) signaling, that regulate longevity[2–4].

However, food is not solely composed of nutrients, as other components are also associated with food, such as volatile odors and various types of nonvolatile, non-nutrient chemicals. Like nutrients, these food components may also affect aging[5]. For example, in *Caenorhabditis elegans*, worms defective in chemosensation show altered lifespan, suggesting a role of chemical cues in lifespan regulation[6,7]; in *Drosophila melanogaster*, odorants from food can inhibit DR longevity[8]. However, it is unclear how non-nutrient chemicals in the food regulate longevity. In particular, it is not known whether and how these non-nutrient food chemicals interact with the brain, and if so, how the brain then engages the rest of the body to alter lifespan. Here, we sought to address these questions in *C. elegans*, a genetic model organism widely used for studying the biology of aging.

Results

Food odors suppress the lifespan of worms under dietary restriction but not those fed ad libitum. Lifespan assays in *C. elegans* are usually conducted on nematode growth medium (NGM) agar plates. Although not as common, lifespan may also be performed in liquid culture. As such, two major types of DR regimens have been developed: (1) solid-phase DR (sDR) assayed on agar plates, and (2) liquid-phase DR (bDR) carried out in liquid culture, each supplied with a reduced amount of bacterial food[9]. Different DR regimens may engage different signaling mechanisms[4,9]. Since sDR has been widely used in the community due to its ease of handling, and because it is rather difficult to expose food odors to worms cultured in liquid, we chose to focus on sDR. In this protocol, bacteria are killed to prevent their further growth[10]. Previous efforts found that application of the supernatant from bacterial culture to the assaying plates shortened the lifespan of worms deprived of food (bacteria deprivation or DD)[11,12]. However, as this protocol did not separate volatile odors from various water-soluble chemicals, it remains unclear whether food odors have an effect on worm longevity.

To directly test the effect of food odors, we developed a protocol to deliver food odors to worms in lifespan assays. To do so, we placed a small piece of NGM agar with a thin lawn of live OP50 bacteria on the lid of the NGM plate (Fig. 1a). As a control, the same size NGM agar piece was placed on the lid but without OP50 bacteria. Worms on the plate did not make direct contact with bacteria on the lid, but were exposed to the odors emitted from these bacteria (Fig. 1a). Exposing such food-derived odors to worms under DR inhibited longevity by ~50%, while exposing food odors to worms fed ad libitum (AL) did not have a notable effect on lifespan (Fig. 1b), revealing a specific effect of food odors on DR longevity.

One potential concern is that food odors might have stimulated feeding, thereby shortening lifespan due to increased food ingestion. This, however, was not the case, as the pharyngeal pumping rate of DR worms was not affected by food odors compared to the control (Fig. 1c and Extended Data Fig. 1a,b). In addition, the amount of ingested bacteria was similar under the two conditions, which was determined by quantifying the fluorescence of worm gut bacteria expressing tdTomato (Fig. 1d,e). Slightly increasing the amount of bacterial food (2×) fed to DR worms stimulated their pharyngeal pumping rate and increased the amount of ingested bacteria in the gut (Fig. 1c–e), yet had no notable effect on lifespan (Extended Data Fig. 1c). By contrast, the inhibitory effect of food odors on the lifespan of DR worms persisted under this condition (Extended Data Fig. 1c). This set of control experiments indicates that the two assays used have the sensitivity to detect small increases in feeding and

[1]College of Life Science and Technology, Key Laboratory of Molecular Biophysics of MOE, Huazhong University of Science and Technology, Wuhan, China. [2]Life Sciences Institute, University of Michigan, Ann Arbor, MI, USA. [3]Department of Molecular and Integrative Physiology, University of Michigan Medical School, Ann Arbor, MI, USA. ✉e-mail: jfliu@mail.hust.edu.cn; shawnxu@umich.edu

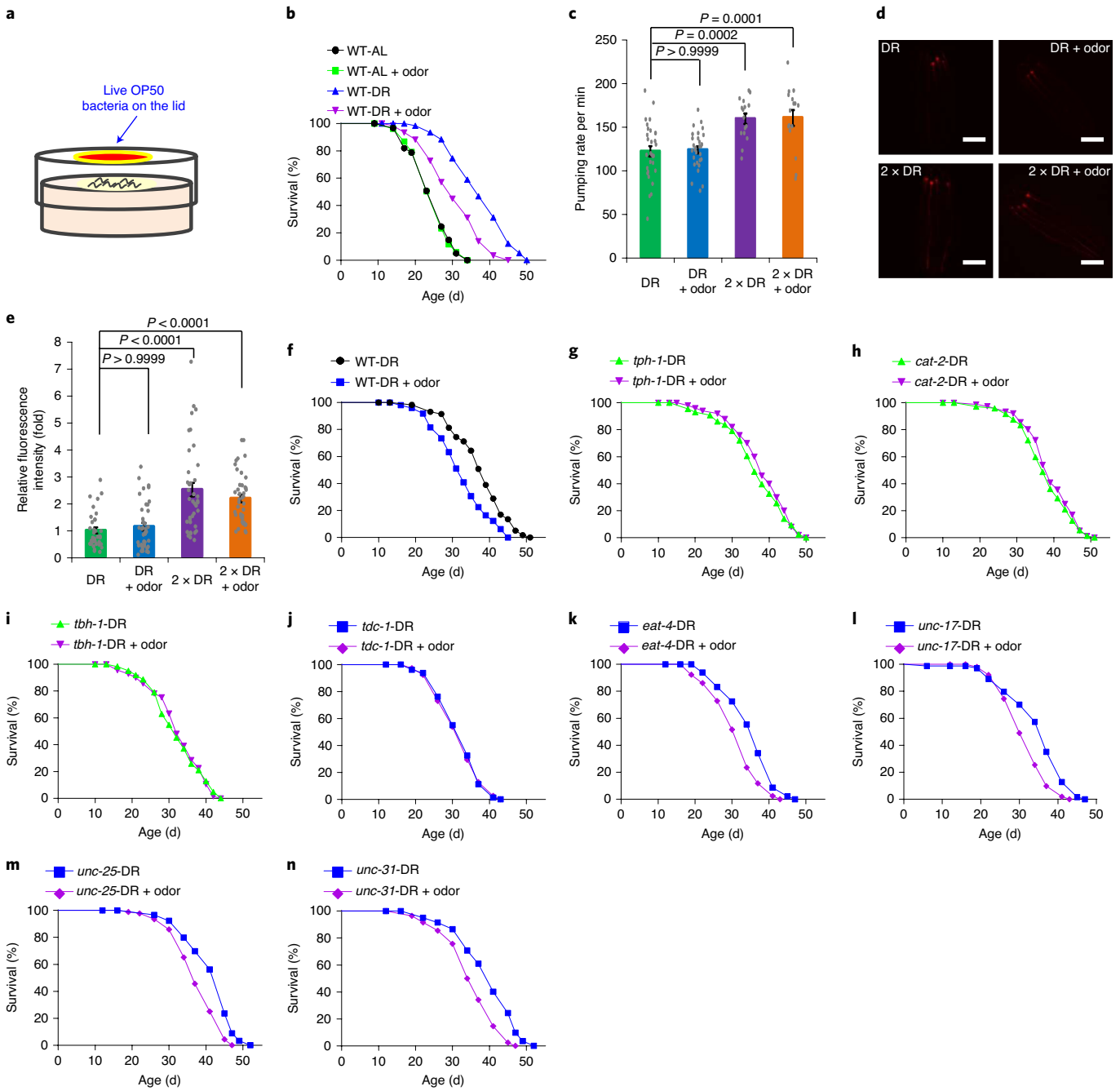

Fig. 1 | Food odors suppress the lifespan of worms under dietary restriction but not those fed AL, and this requires neurotransmission. a–c, Food-derived odors shortened the lifespan of worms under DR, but not those fed AL. **a**, Schematic describing the assay. **b**, Lifespan curves. **c**, Food odors did not change the pumping rate of worms under DR. Pumping rate was counted at 1 h after worms were transferred to the DR assaying plates. 2 × DR, twice the amount of bacterial food. $n = 30$ (DR), 30 (DR + odor), 16 (2 × DR) and 16 (2 × DR + odor) biologically independent animals. **d**,**e**, Food odors did not change the amount of bacteria ingested by worms under DR. tdTomato-expressing OP50 bacteria were used as the food source. Scale bars, 200 µm. **d**, Sample images. **e**, Bar graph. $n = 34$ (DR), 40 (DR + odor), 40 (2 × DR) and 40 (2 × DR + odor) biologically independent animals. **f–n**, Food odors shortened the lifespan of wild-type (WT) (**f**), *eat-4* mutant (**k**), *unc-17* mutant (**l**), *unc-25* mutant (**m**) and *unc-31* mutant (**n**) worms under the DR condition. However, loss of *tph-1* (**g**), *cat-2* (**h**), *tbh-1* (**i**) or *tdc-1* (**j**) blocked the ability of food odors to suppress DR longevity. Data are presented as the mean ± s.e.m. *P* values were calculated using one-way analysis of variance (ANOVA) with Bonferroni's test. See Supplementary Table 1 for lifespan statistics.

food intake that would have been induced by food odors. We thus conclude that food odors inhibit longevity in a DR-dependent manner in *C. elegans*.

Food odor-induced suppression of DR longevity requires neurotransmission. How do food odors suppress DR longevity? As odors are usually detected by the nervous system, which involves neurotransmission, we first asked whether and which types of neurotransmission mediate the odor effect. By screening different neurotransmission mutants, we found that mutations abolishing the synthesis of serotonin (*tph-1*), dopamine (*cat-2*), octopamine (*tbh-1*) or tyramine (*tdc-1*) all prevented food odors from inhibiting DR longevity (Fig. 1f–j), indicating a requirement of these neurotransmitters. Other neurotransmitter mutants such as *eat-4*

(glutamate), *unc-17* (acetylcholine), *unc-25* (γ-aminobutyric acid) and *unc-31* (neuropeptides) did not exhibit a notable defect (Fig. 1k–n). These results raise the possibility that serotonin, dopamine and octopamine/tyramine neurons may form a chemosensory circuit to sense and process odor signals to inhibit DR longevity.

ADF, CEP and RIC neurons form an olfactory circuit mediating odor-induced suppression of DR longevity. Among serotonin, dopamine and octopamine/tyramine neurons, only ADF serotonin neurons are chemosensory neurons[13]; the other major type of serotonin neuron (NSM) is classified as a motor neuron[14], while dopamine neurons (CEP, ADE and PDE) are mechanosensory neurons[15–17], and octopamine/tyramine neurons (RIC and RIM) are interneurons[18]. As ADF neurons are known to sense volatile odors[19], ADF neurons might function as the olfactory neurons in the circuit to sense food odors. To test this, we recorded the activity of both ADF and NSM serotonin neurons in response to food odors by calcium imaging. ADF neurons from DR worms responded robustly to medium containing odors from OP50 bacterial food (Fig. 2a,d). Strikingly, ADF neurons from AL-fed worms responded very weakly to food odors (Fig. 2a,d), revealing a DR-specific effect. By contrast, food odors evoked no notable response in NSM serotonin neurons (Extended Data Fig. 2b,c), suggesting that NSM neurons are not part of the circuit. To test whether ADF neurons sense food odors cell autonomously, we repeated the imaging experiment in *unc-13* and *unc-31* mutants, and obtained a similar result (Fig. 2b,d). Mutations in *unc-13* and *unc-31* block neurotransmitter release from synaptic vesicles and dense core vesicles, respectively[20,21]. Thus, ADF neurons likely responded to food odors cell autonomously, suggesting that these chemosensory neurons act as primary olfactory sensory neurons to sense food odors in DR worms.

We then asked whether ADF neurons are important for mediating the inhibitory effort of food odors on DR longevity. We ablated the output of ADF neurons by expressing TeTx (tetanus toxin) as a transgene specifically in these neurons. TeTx cleaves synaptobrevin, an essential SNARE subunit, to block exocytosis[22]. Ablating the output of ADF neurons, but not NSM neurons, abolished the effect of food odors (Fig. 2m and Extended Data Fig. 2o), indicating that ADF neurons are required for food odors to suppress DR longevity. These data, together with our calcium imaging results, suggest that ADF chemosensory neurons act as primary olfactory sensory neurons to sense food odors for suppression of longevity in DR worms.

Using the same strategy, we interrogated the potential roles of dopamine neurons (CEP, ADE and PDE), octopamine neurons (RIC) and tyramine neurons (RIM) in the circuit. CEP dopamine neurons responded robustly to food odors in a DR-dependent manner (Fig. 2e,h), while ADE and PDE dopamine neurons did not (Extended Data Fig. 2g–i). Interestingly, RIC neurons also displayed DR-dependent calcium response to food odors, except that food odors inhibited rather than stimulated their activity (Fig. 2i–l). These results suggest that CEP and RIC neurons are part of the circuit. One notable observation is that, while different subcompartments of ADF and RIC neurons (dendrites, soma and axon for ADF; soma and processes for RIC) all responded similarly to food odors (Extended Data Fig. 2a,c,j,l), in CEP neurons, only the dendrites responded to food odors in a DR-dependent manner (Extended Data Fig. 2d–f). This is not surprising, as many worm neurons show compartmentalized calcium responses[23,24]. By contrast, RIM neurons exhibited no specificity toward DR, as these neurons from DR and AL-fed worms responded similarly to food odors (Extended Data Fig. 2k,l), suggesting that RIM neurons are not part of the circuit. These calcium imaging results demonstrate that, in addition to ADF neurons, CEP and RIC neurons are also part of the circuit. Consistent with this model, blocking the output of CEP and RIC neurons using a TeTx transgene eliminated the inhibitory effect of food odors on DR longevity (Fig. 2n–o), indicating that CEP and RIC neurons are required for food odors to suppress lifespan in DR worms. We thus conclude that ADF, CEP and RIC neurons are essential components of an olfactory circuit that senses and processes odor signals from food to suppress longevity in DR worms.

We then sought to map the position of ADF, CEP and RIC neurons in the circuit. Given our data showing that ADF neurons are the primary olfactory neurons sensing food odors, CEP and RIC neurons would be expected to act downstream of ADF in the circuit. If so, blocking the output of the upstream ADF sensory neurons would abolish the sensitivity of the downstream CEP and RIC neurons to food odors. This appears to be the case: blunting the output of ADF with a TeTx transgene rendered both CEP and RIC neurons insensitive to food odors (Fig. 2f,h,j,l); so did mutations in *tph-1* that abolished serotonin release from ADF neurons (Fig. 2f,h,j,l). On the other hand, eliminating the output of the downstream neurons CEP and RIC using mutations in *cat-2* (blocking dopamine release from CEP) or *tbh-1* (blocking octopamine release from RIC), respectively, had no effect on the response of ADF to food odors (Fig. 2c,d). This set of experiments places ADF neurons upstream of CEP and RIC neurons.

Fig. 2 | Food odors act on an olfactory circuit, comprising ADF, CEP and RIC neurons, to suppress DR longevity. a, ADF neurons from DR worms responded robustly to medium containing odors from OP50 bacterial food, while very weak, if any, calcium response was evoked by food odors in ADF neurons from AL-fed worms. GCaMP6f was expressed as a transgene in ADF neurons under the *tph-1(L)* promoter. DsRed was coexpressed to enable ratiometric imaging. Solid lines indicate responses of GCaMP over time (measured as $\Delta R/R$). **b**, Food odor-evoked calcium response in AFD neurons remained normal in *unc-13* and *unc-31* mutant worms. **c**, Blocking dopamine signaling (using *cat-2* mutation) or octopamine signaling (using *tbh-1* mutation) did not notably affect food odor-evoked calcium response in ADF neurons. **d**, Bar graph summarizing the data in **a**, **b** and **c**. $n = 8$ (WT-AL), 10 (WT-DR), 10 (*unc-13*-AL), 10 (*unc-13*-DR), 10 (*unc-31*-AL), 11 (*unc-31*-DR), 11 (*cat-2*-AL), 11 (*cat-2*-DR), 10 (*tbh-1*-AL) and 10 (*tbh-1*-DR) biological independent animals. **e**, CEP neurons from DR worms but not AL-fed worms responded to food odors. To facilitate dendrite imaging, we expressed myr-GCaMP6f (membrane targeted) in CEP using the *dat-1* promoter. Note that the *dat-1* promoter also drives expression in ADE and PDE dopamine neurons. **f**, Blocking serotonin signaling (using either *tph-1* mutation or *ADF::TeTx* transgene) eliminated CEP calcium response evoked by food odors. **g**, Blocking octopamine signaling (using *tbh-1* mutation) had no effect on CEP calcium response evoked by food odors. **h**, Bar graph summarizing data in **e**, **f** and **g**. $n = 11$ (WT-AL), 9 (WT-DR), 13 (*tph-1*-AL), 13 (*tph-1*-DR), 10 (*ADF::TeTx*-AL), 11 (*ADF::TeTx*-DR), 10 (*tbh-1*-AL) and 10 (*tbh-1*-DR) biological independent animals. **i**, RIC neurons from DR worms but not AL-fed worms responded to food odors. The *tbh-1* promoter was used to drive transgene expression in RIC. **j**,**k**, Blocking serotonin signaling (using *tph-1* mutation or *ADF::TeTx* transgene (**j**)) or inhibiting dopamine signaling (using *cat-2* mutation or *CEP::TeTx* transgene (**k**)) abolished RIC calcium response evoked by food odors. **l**, Bar graph summarizing the data in **i**, **j** and **k**. $n = 11$ (WT-AL), 14 (WT-DR), 12 (*tph-1*-AL), 14 (*tph-1*-DR), 8 (*ADF::TeTx*-AL), 8 (*ADF::TeTx*-DR), 13 (*cat-2*-AL), 15 (*cat-2*-DR), 8 (*CEP::TeTx*-AL) and 9 (*CEP::TeTx*-DR) biological independent animals. **m**–**o**, Blocking the output from ADF (**m**), CEP (**n**) and RIC (**o**) neurons using *TeTx* transgene abrogated the ability of food odors to suppress DR longevity. A fragment of the *bas-1* promoter (*bas-1*(*prom7*)), *dat-1* promoter and *tbh-1* promoter was used to drive *TeTx* expression in ADF, CEP and RIC neurons, respectively. Data are presented as the mean ± s.e.m. Shading along the calcium imaging traces represents error bars (±s.e.m). *P* values were calculated with one-way ANOVA with Bonferroni's test. See Supplementary Table 1 for lifespan statistics.

Using a similar strategy, we tested CEP and RIC neurons. While blocking the output of CEP neurons (using a TeTx transgene and *cat-2* mutation) abrogated the odor sensitivity of RIC neurons (Fig. 2k,l), inhibiting the output of RIC neurons (using *tbh-1* mutation) had no effect on the sensitivity of CEP neurons to food odors (Fig. 2g,h). This places CEP upstream of RIC neurons. As food odors stimulated ADF and CEP neurons but inhibited RIC neurons, this suggests a circuit mechanism by which food odors suppress DR longevity by stimulating ADF and CEP neurons to inhibit RIC neurons (Fig. 3l). Although CEP neurons are mechanosensory neurons, considering that they act downstream of ADF, these CEP neurons may in fact function as interneurons in the circuit.

Molecular mechanisms by which the olfactory circuit senses and processes odor signals. To gain a molecular understanding of how the olfactory circuit senses and processes odor signals from food, we next identified the receptors that act in each neuron to sense and process odor signals. Olfactory transduction in *C. elegans* sensory neurons is a G-protein-mediated process that culminates in the opening of downstream transduction channels, leading to sensory neuron activation[13]. We thus examined the G protein ODR-3 and the transduction channel subunit OCR-2 known to function in ADF sensory neurons to mediate chemosensation[13,25]. Mutations in both *odr-3* and *ocr-2* not only abolished calcium response to food odors in ADF neurons (Fig. 3a–c), but also the ability of food odors

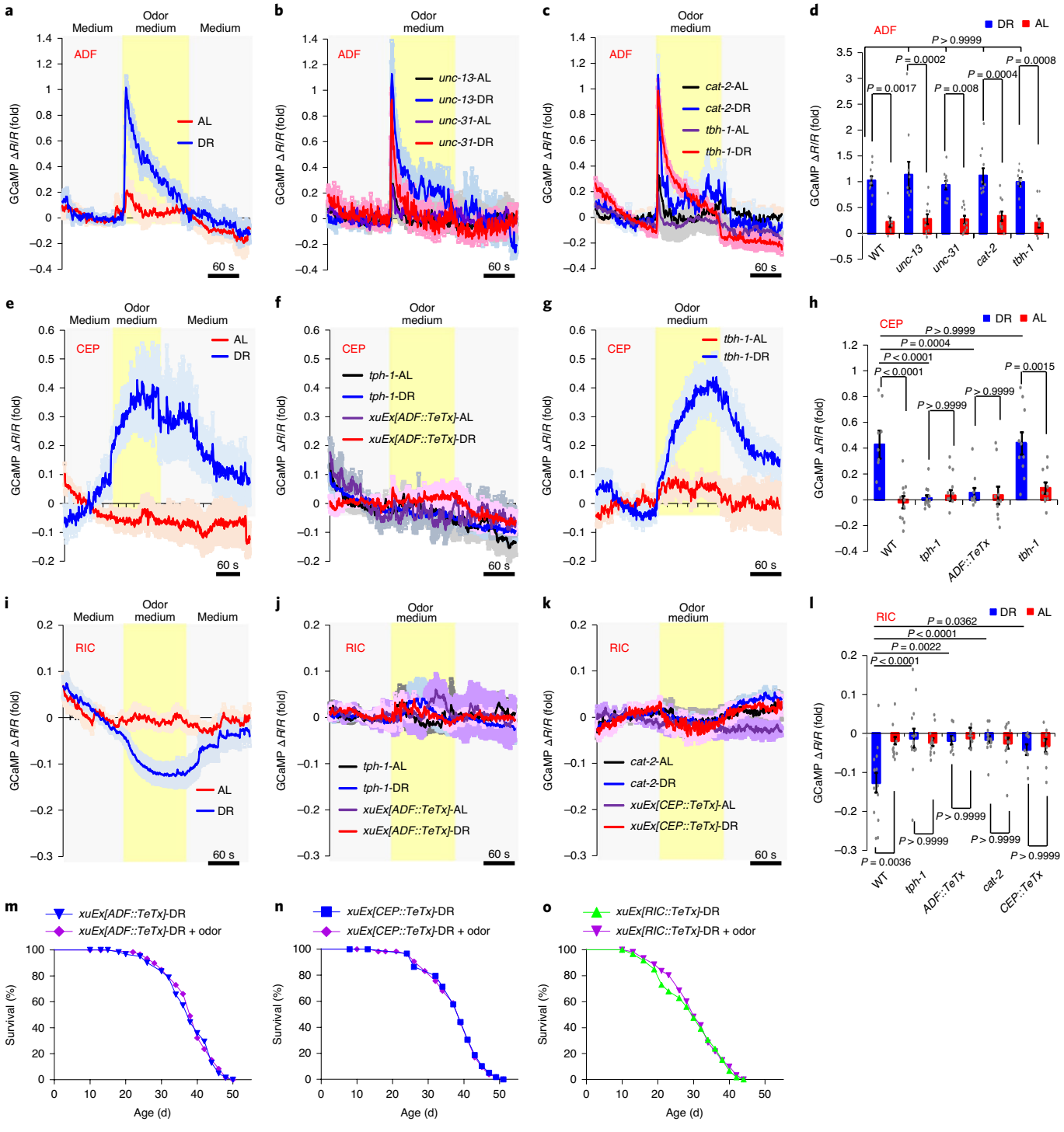

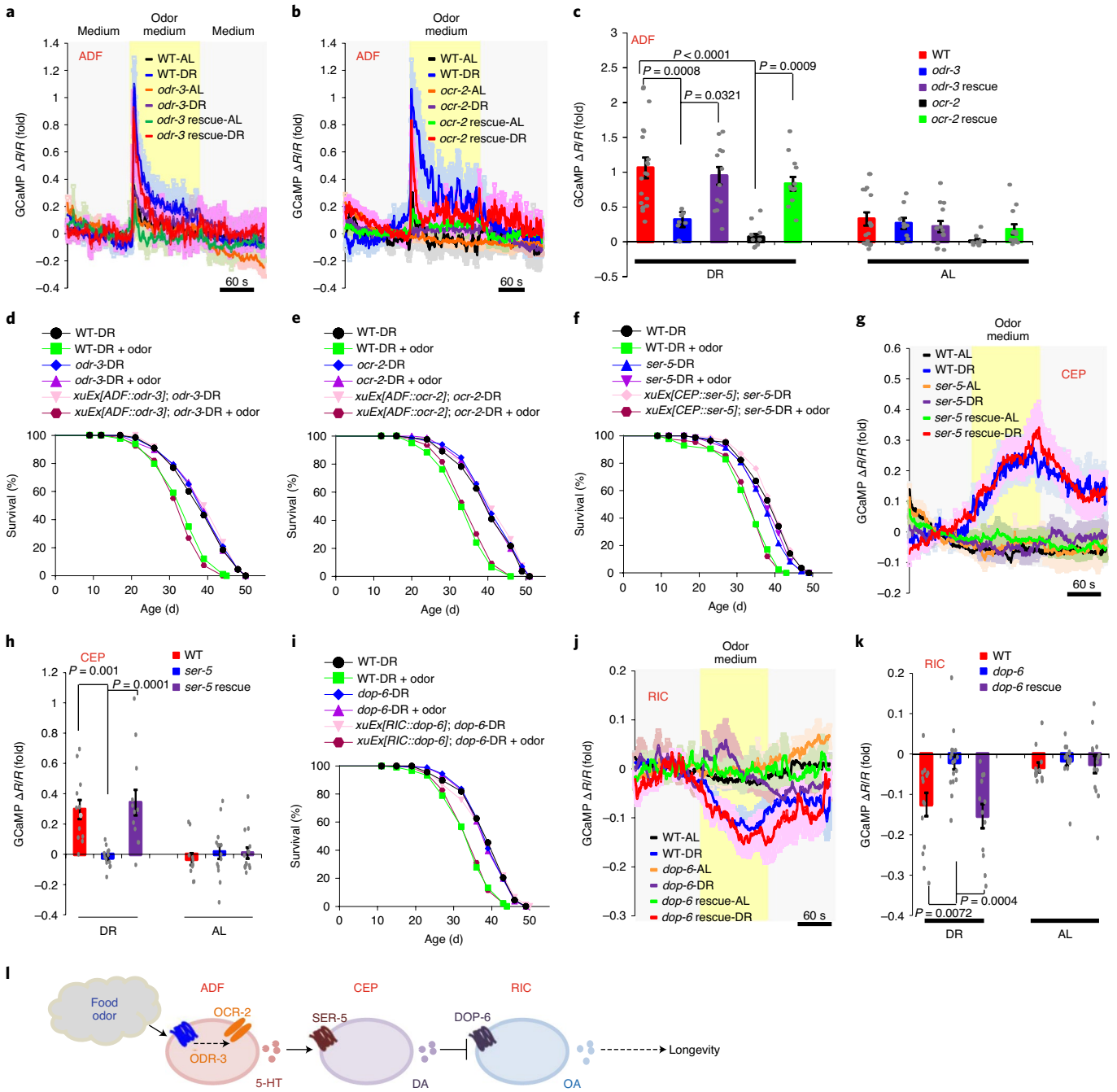

Fig. 3 | The molecular basis by which the olfactory circuit senses and processes odor signals from food. a–c, Mutations in *odr-3* (**a**) and *ocr-2* (**b**) abolished food odor-evoked calcium response in ADF neurons, a phenotype rescued by transgenic expression of WT *odr-3* and *ocr-2* genes in ADF neurons. A fragment of the *bas-1* promoter (*bas-1*(*prom7*)) was used to drive expression of *odr-3* and *ocr-2* cDNA specifically in ADF neurons. **c**, Bar graph summarizing the data in **a** and **b**. $n = 17$ (WT-AL), 20 (WT-DR), 9 (*odr-3*-AL), 8 (*odr-3*-DR), 13 (*odr-3* rescue-AL), 12 (*odr-3* rescue-DR), 9 (*ocr-2*-AL), 9 (*ocr-2*-DR), 13 (*ocr-2* rescue-AL) and 13 (*ocr-2* rescue-DR) biological independent animals. **d**,**e**, Mutations in *odr-3* (**d**) and *ocr-2* (**e**) prevented food odors from suppressing DR longevity, a phenotype rescued by transgenic expression of WT *odr-3* and *ocr-2* cDNA in ADF neurons. **f**, Loss of *ser-5* eliminated the ability of food odors to suppress DR longevity, a phenotype rescued by transgenic expression of *ser-5* cDNA in CEP neurons using the *dat-1* promoter. **g**, Loss of *ser-5* abolished CEP calcium response evoked by food odors, a defect rescued by transgenic expression *ser-5* cDNA in CEP neurons. **h**, Bar graph summarizing the data in **g**. $n = 11$ (WT-AL), 12 (WT-DR), 14 (*ser-5*-AL), 13 (*ser-5*-DR), 15 (*ser-5* rescue-AL) and 12 (*ser-5* rescue-DR) biological independent animals. **i**, Loss of *dop-6* prevented food odors from suppressing DR longevity, a phenotype rescued by transgenic expression of *dop-6* cDNA in RIC neurons. **j**, Loss of *dop-6* abolished RIC calcium response evoked by food odors, a defect rescued by transgenic expression of *dop-6* cDNA in RIC neurons. **k**, Bar graph summarizing the data in **j**. $n = 12$ (WT-AL), 14 (WT-DR), 15 (*dop-6*-AL), 17 (*dop-6*-DR), 14 (*dop-6* rescue-AL) and 12 (*dop-6* rescue-DR) biological independent animals. **l**, Schematic of the olfactory circuit that senses and processes odor signals from food to suppress DR longevity. Data are presented as the mean ± s.e.m. Shading along the calcium imaging traces represents error bars (±s.e.m). *P* values were calculated using one-way ANOVA with Bonferroni's test. See Supplementary Table 1 for lifespan statistics. 5-HT, serotonin; DA, dopamine; OA, octopamine.

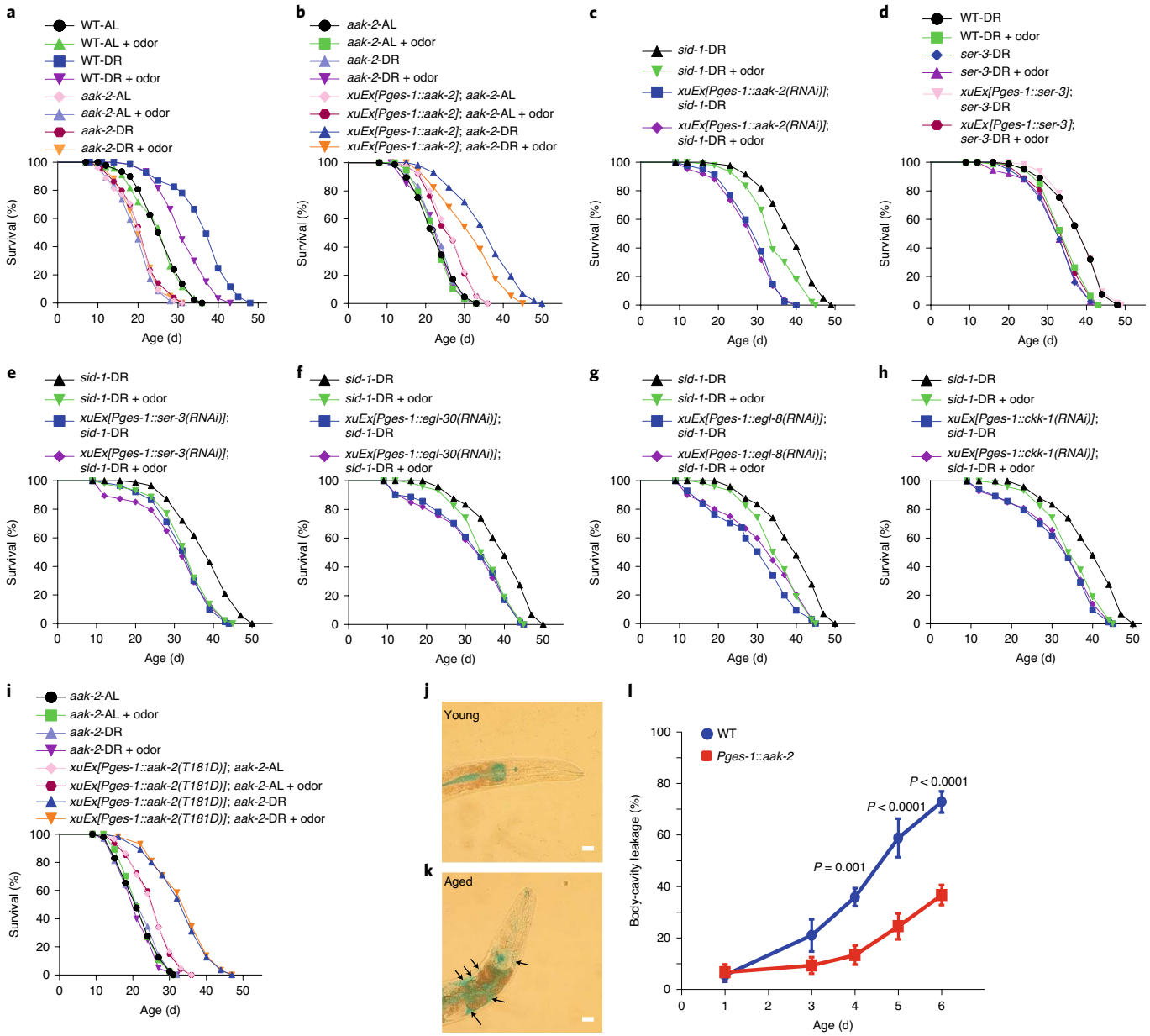

Fig. 4 | The olfactory circuit signals the intestine to regulate the energy sensor AAK-2/AMPK via Gq-PLCβ-CaMKK-dependent norepinephrine signaling. a, *aak-2* mutant worms were completely insensitive to DR and food odors. **b**, Transgenic expression of WT *aak-2* gene in the intestine rescued both the longevity and odor sensitivity phenotypes in *aak-2* mutant worms. **c**, RNAi of *aak-2* in the intestine abolished the ability of food odors to suppress DR longevity. dsRNA against *aak-2* was expressed as a transgene specifically in the intestine using the *ges-1* promoter. All experiments were carried out in a *sid-1* mutant background where the systemic effect of RNAi is absent. **d**, Loss of *ser-3* abolished the ability of food odors to suppress DR longevity, a phenotype rescued by transgenic expression of WT *ser-3* gene in the intestine using the *ges-1* promoter. **e**, Intestine-specific RNAi of *ser-3* by a dsRNA transgene prevented food odors from suppressing DR longevity. **f**–**h**, Intestine-specific RNAi of *egl-30*/Gq (**f**), *egl-8*/PLCβ (**g**) or *ckk-1*/CaMKK (**h**) by dsRNA transgenes abolished the ability of food odors to suppress DR longevity. Experiments in **f**, **g** and **h** share the same *sid-1* control curves, as these were performed at the same time. **i**, *aak-2*(T181D) transgene rescued the DR longevity defect but not the odor sensitivity defect of *aak-2* mutant worms. **j**–**l**, Intestinal expression of AAK-2/AMPK slowed down the age-dependent decline in intestinal barrier function. The blue dye (FD&C blue), which is impermeable to the intestine epithelium, was taken up into the intestine by the worm. The dye was confined inside the intestinal lumen in young worms; but as worms aged, the dye leaked into the body cavity. Worms were cultured at 25 °C. **j**, Young WT worm (day 1). **k**, Aged WT worm (day 6), showing leakage of the dye into the body cavity. Arrows point to the dye outside of the intestine. Scale bars, 25 μm. **l**, Graph showing that the intestinal *aak-2* transgene *Pges-1::aak-2* slowed down the age-dependent dye leakage. The percentage of worms showing body-cavity dye leakage was quantified. Each data point was derived from ten worms and repeated five times. Data are presented as the mean ± s.e.m. *P* values were calculated using one-way ANOVA with Bonferroni's test. See Supplementary Table 1 for lifespan statistics.

to suppress DR longevity (Fig. 3d,e). Both phenotypes were rescued by transgenic expression of wild-type *odr-3* and *ocr-2* genes in ADF neurons (Fig. 3a–e), demonstrating that ODR-3 and OCR-2 act in ADF neurons to sense food odors. Additional evidence came from cell-specific RNA-mediated interference (RNAi) knockdown experiments, where we expressed double-stranded RNA (dsRNA) of *odr-3*

or *ocr-2* as a transgene specifically in ADF neurons. RNAi of *odr-3* and *ocr-2* in ADF neurons abolished their sensitivity to food odors (Extended Data Fig. 2m,n), providing further evidence that ODR-3 and OCR-2 act in ADF neurons to sense food odors. These experiments are also consistent with the notion that ADF neurons are primary olfactory sensory neurons[19].

ADF neurons are serotonergic. Given that CEP neurons act downstream of ADF neurons, we reasoned that a serotonin receptor might act in CEP neurons to transmit odor signals by responding to serotonin released from ADF neurons. We thus examined all the five serotonin receptor genes encoded by the worm genome: *ser-1*, *ser-4*, *ser-5*, *ser-7* and *mod-1* (ref. [26]). Mutations in *ser-5*, but not the other four serotonin receptor genes, blocked the ability of food odors to suppress DR longevity, a phenotype that was rescued by transgenic expression of wild-type *ser-5* gene in CEP neurons (Fig. 3f and Extended Data Fig. 3a–d). Thus, SER-5 may function as the serotonin receptor in CEP neurons to transmit odor signals. In support of this idea, no food odor-evoked calcium response in CEP neurons was detected in *ser-5* mutant worms, and this phenotype was rescued by a *ser-5* transgene expressed in CEP neurons (Fig. 3g,h). These results identify SER-5 as the serotonin receptor that acts in CEP neurons to transmit odor signals in the circuit.

CEP neurons are dopaminergic. We thus hypothesized that a dopamine receptor may act in the downstream RIC neurons to transmit odor signals by responding to dopamine released from CEP neurons. By screening mutants of all six dopamine receptor genes encoded by the worm genome: *dop-1*, *dop-2*, *dop-3*, *dop-4*, *dop-5* and *dop-6* (ref. [26]), we found that food odors lost the ability to suppress DR longevity in *dop-6* but not the other five *dop* mutant worms (Fig. 3i and Extended Data Fig. 4a–e). Similarly, RIC neurons in *dop-6* mutant worms lost the ability to respond to food odors in the calcium imaging assay (Fig. 3j,k). Both phenotypes were rescued by transgenic expression of wild-type *dop-6* gene in RIC neurons (Fig. 3i–k). Thus, DOP-6 may function as the dopamine receptor in RIC neurons to transmit odor signals in the circuit.

Together, our data suggest a model that food odors suppress DR longevity via an olfactory circuit comprising three pairs of neurons: ADF, CEP and RIC (Fig. 3l). In this circuit, we suggest that ADF neurons function as primary sensory neurons to sense food odors through a G-protein-mediated transduction mechanism; ADF neurons then stimulate CEP neurons, which in turn inhibit RIC neurons; SER-5 and DOP-6 function in CEP and RIC neurons to transmit odor signals by responding to the neurotransmitter serotonin and dopamine released from upstream neurons, respectively (Fig. 3l). As food odors inhibit RIC neurons to suppress DR longevity, this suggests that the normal output of RIC neurons is to promote longevity. If so, then inhibiting the output of RIC neurons should mimic the inhibitory effect of food odors on DR longevity. Indeed, inhibiting the output of RIC neurons with a TeTx transgene shortened DR longevity (Extended Data Fig. 2p), providing further evidence that food odors suppress DR longevity by inhibiting the output of RIC octopamine neurons.

The olfactory circuit signals the intestine to regulate the energy sensor AMPK. We then wondered how the olfactory circuit engages the rest of the animal body to regulate DR longevity. As DR longevity pathways all converge on nutrient signaling[2–4], we first asked which nutrient signaling pathway underlies DR longevity in our lifespan assay. AMPK and mTOR signaling are the two primary nutrient signaling that regulate DR longevity in worms[2,3]. Consistent with previous work[10], we found that loss of the *C. elegans* AMPKα ortholog AAK-2 abolished the ability of DR to extend lifespan (Fig. 4a), demonstrating that AAK-2 is required for DR longevity. This supports the notion that AMPK mediates the longevity under the sDR regimen[10]. Notably, *aak-2* mutant worms were also insensitive to food odors (Fig. 4a), indicating a requirement of AMPK for food odors to suppress DR longevity. By contrast, DR longevity persisted in *raga-1* and *rict-1* mutant worms (Extended Data Fig. 5a,c), which were deficient in mTORC1 and mTORC2 signaling, respectively[27], and these two mutants also remained sensitive to food odors (Extended Data Fig. 5b,d). Thus, both DR longevity and its sensitivity to food odors require AMPK but not mTOR signaling in our DR regimen. Notably, transgenic expression of wild-type *aak-2* gene in the intestine rescued both the longevity and odor sensitivity defects in *aak-2* mutant worms (Fig. 4b). By contrast, expression of *aak-2* as a transgene in neurons only had a slight rescue effect on the longevity defect (Extended Data Fig. 5e). Neuronal expression of *aak-2* also failed to rescue the odor sensitivity defect in *aak-2* mutant worms. Thus, AAK-2 primarily acts in the intestine. Additional evidence came from an RNAi experiment, in which we knocked down *aak-2* expression in the intestine by expressing dsRNA against *aak-2* as a transgene specifically in the intestine, and found that it blocked the ability of food odors to suppress DR longevity (Fig. 4c). This experiment was conducted in a *sid-1* mutant background to restrict RNAi to the tissue of interest[28]. Together, these results suggest that the olfactory circuit signals the intestine to regulate the energy sensor AMPK to suppress DR longevity, revealing a brain–gut signaling axis.

Given that AAK-2/AMPK expression in the intestine extended lifespan (Extended Data Fig. 6a), we wondered if it could also promote the health of the intestine. A primary function of the intestine epithelium is to form a selective barrier that allows it to absorb nutrients, ions and water but remain impermeable to toxic substances and microorganisms[29,30]. Like other animals[29,31], the barrier function of the intestine in *C. elegans* declines with age progressively, which renders the intestine of aged worms permeable to otherwise impermeable chemicals, resulting in their leakage into the body cavity[30] (Fig. 4j,k). Intestinal expression of AAK-2 greatly slowed down the age-dependent decline in the intestinal barrier function (Fig. 4l), indicating that AMPK can promote the health of the intestine.

Gq-PLCβ-CaMKK-dependent octopamine signaling regulates AMPK in the intestine. How does the olfactory circuit signal the intestine to regulate AMPK? As RIC neurons are octopamine neurons acting downstream in the circuit (Fig. 3l), we reasoned that RIC neurons might signal the intestine via octopamine. Consistent with this model, food odors failed to suppress DR longevity in *tbh-1* mutant worms deficient in octopamine production (Fig. 1i). We then attempted to identify the octopamine receptor that functions in the intestine to transmit odor signals to regulate AMPK. Among all three worm octopamine receptor genes (that is, *ser-3*, *ser-6* and *octr-1*)[26], loss of *ser-3* but not the other two receptor genes abrogated the ability of food odors to suppress DR longevity (Fig. 4d and Extended Data Fig. 5f,g). Transgenic expression of wild-type

Fig. 5 | Octopamine signaling in the intestine promotes lifespan and stimulates AMPK phosphorylation via a Gq-PLCβ-CaMKK-dependent mechanism. **a–d**, Transgenic expression of the octopamine receptor SER-3 in the intestine (*Pges-1::ser-3*) extended lifespan under normal conditions (**a**), and this lifespan-extending effect was blocked by intestine-specific RNAi of *egl-30*/Gq (**a**), *egl-8*/PLCβ (**b**), *ckk-1*/CaMKK (**c**) and *aak-2* (**d**) with corresponding dsRNA transgenes. Experiments in **b** and **c** share the same *sid-1* control curves, as these were performed at the same time. **e**, Transgenic expression of *ser-3* in the intestine (*Pges-1::ser-3*) stimulates AAK-2/AMPK phosphorylation. Samples collected from *aak-2* mutant worms were used to demonstrate the specificity of the antibody. Actin (ACT-1) was used as a loading control. N2, wild type. **f–h**, Loss of *egl-30*/Gq (**f**), *egl-8*/PLCβ (**g**) or *ckk-1*/CaMKK (**h**) inhibits SER-3-dependent stimulation of AAK-2/AMPK phosphorylation. See Supplementary Table 1 for lifespan statistics.

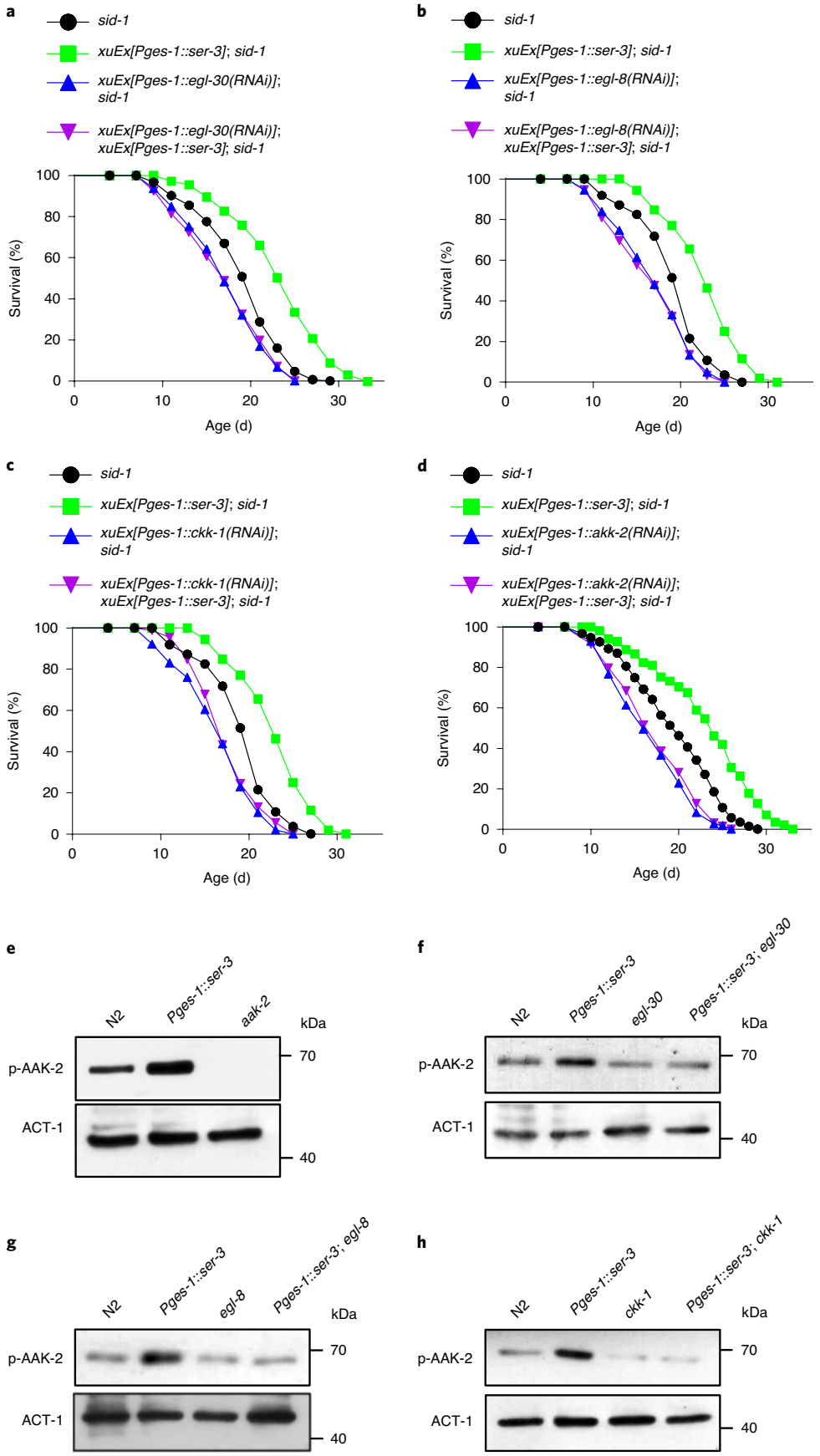

ser-3 gene in the intestine rescued the odor sensitivity defect in *ser-3* mutant worms (Fig. 4d). In addition, RNAi of *ser-3* specifically in the intestine of wild-type worms recapitulated the *ser-3* mutant phenotype (Fig. 4e). These data identify SER-3 as the octopamine receptor that acts in the intestine to transmit signals from the olfactory circuit to regulate AMPK.

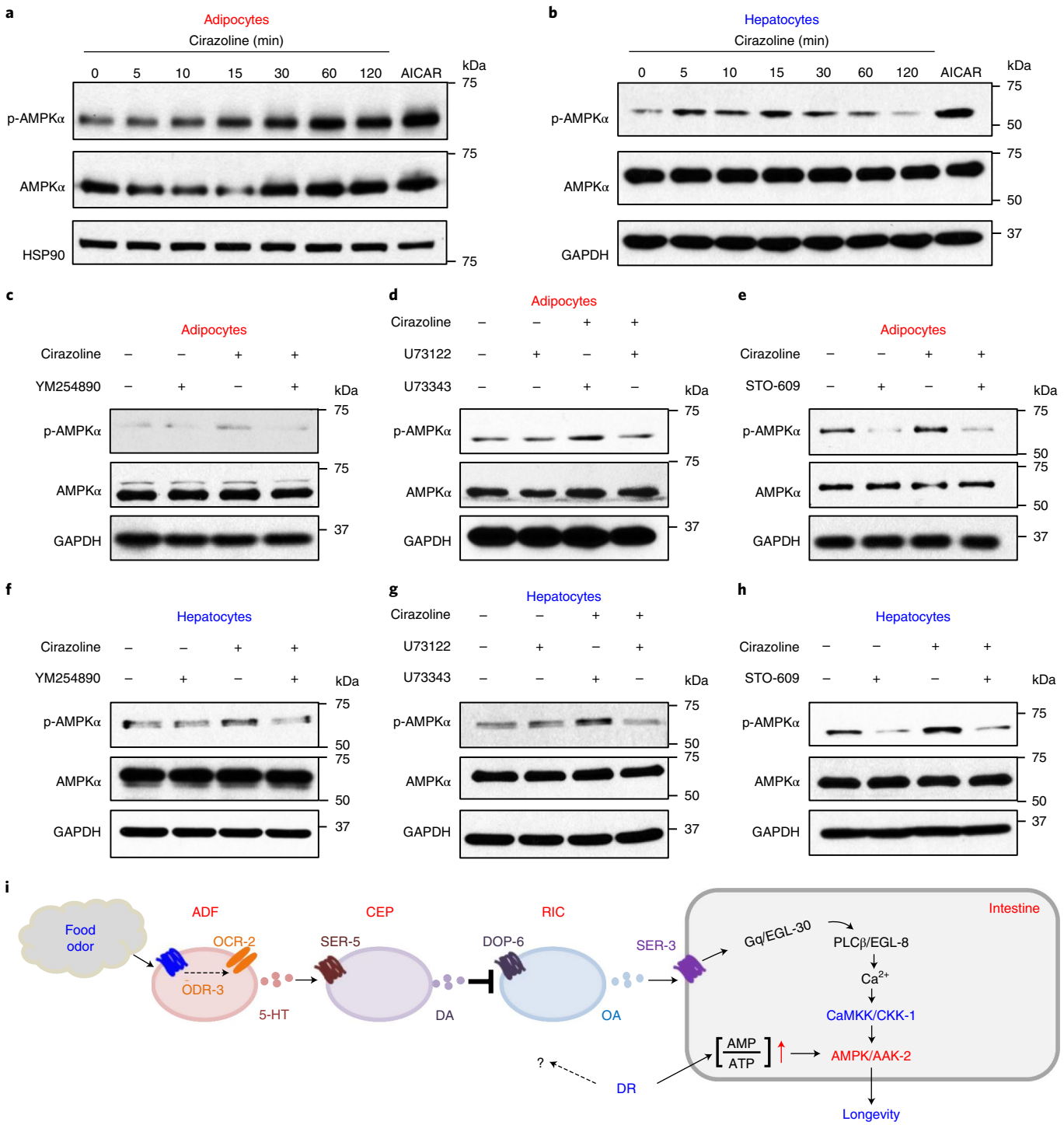

Fig. 6 | Activation of norepinephrine signaling stimulates AMPK via a Gq-PLCβ-CaMKK-dependent mechanism in mouse primary cells. a, Selective activation of α1A-adrenergic receptor activated AMPK in mouse primary subcutaneous adipocytes. Cirazoline (100 μM), a selective agonist for the α1A-adrenergic receptor, stimulated the phosphorylation of the Thr 172 site in AMPKα. AICAR (500 μM; 15 min), an AMPK activator, was used as a positive control. HSP90, heat-shock protein 90. **b**, Selective activation of the α1A-adrenergic receptor activated AMPK in mouse primary hepatocytes. Cirazoline (100 μM) stimulated the phosphorylation of Thr 172 site in AMPKα. AICAR (500 μM; 15 min) was used as a positive control. **c**–**e**, Inhibition of Gq (**c**), PLCβ (**d**) or CaMKK (**e**) abolished cirazoline-induced (100 μM; 60 min) phosphorylation of the Thr 172 site in AMPKα in mouse primary subcutaneous adipocytes. Cells were pretreated with the following inhibitors for 30 min: the Gq inhibitor YM254890 (25 μM), the PLC inhibitor U73122 (5 μM), U73343 (5 μM; that is, an inactive analog of U73122) and the CaMKK inhibitor STO-609 (5 μM). **f**–**h**, Inhibition of Gq (**f**), PLCβ (**g**) or CaMKK (**h**) abolished cirazoline-induced (100 μM; 15 min) phosphorylation of the Thr 172 site in AMPKα in mouse primary hepatocytes. Cells were pretreated with the following inhibitors for 30 min: YM254890 (25 μM), U73122 (5 μM), U73343 (5 μM) and STO-609 (5 μM). **i**, Schematic model.

The question arises as to how the octopamine receptor SER-3 regulates AMPK in the intestine. SER-3 is coupled to Gq protein -phospholipase Cβ (Gq-PLCβ)-mediated calcium signaling[32]. We thus examined the worm Gq ortholog EGL-30 and PLCβ ortholog EGL-8. RNAi of *egl-30* and *egl-8* specifically in the intestine prevented food odors from suppressing DR longevity (Fig. 4f,g),

indicating a requirement for Gq and PLCβ in the pathway. Then how does Gq-PLCβ couple SER-3 to AMPK? AMPK activation requires phosphorylation of its catalytic alpha subunit by an AMPK kinase[33]. Among the three AMPK kinases CaMKK, LKB1 and TAK1, CaMKK is the only one that is activated by calcium signaling[33]. As Gq-PLCβ activation triggers calcium signaling[34], CaMKK emerges as a candidate AMPK kinase that couples SER-3-Gq-PLCβ to AMPK. Indeed, RNAi of the worm CaMKK gene *ckk-1* specifically in the intestine prevented food odors from suppressing DR longevity (Fig. 4h), while RNAi of the other two putative AMPK kinase genes *par-4*/LKB1 and *mom-4*/TAK1 did not (Extended Data Fig. 5h,i). This result suggests that CKK-1/CaMKK is an AMPK kinase that acts downstream of Gq-PLCβ to activate AMPK. As a complementary approach, we examined *egl-30*, *egl-8* and *ckk-1* mutant worms, and found that they all lost the sensitivity to food odors in the lifespan assay, a phenotype that was rescued by transgenic expression of wild-type *egl-30*, *egl-8* and *ckk-1* genes in the intestine, respectively (Extended Data Fig. 5j–l). Together, these observations suggest that the octopamine receptor SER-3 regulates AMPK in the intestine via a Gq-PLCβ-CaMKK-dependent mechanism.

To provide additional evidence, we overexpressed the octopamine receptor SER-3 as a transgene in the intestine, and found that it extended lifespan under normal conditions (Fig. 5a), suggesting that activation of octopamine signaling in the intestine promotes longevity. This is also consistent with our observation that the output of RIC octopamine neurons in the olfactory circuit is to promote longevity. Importantly, the SER-3-dependent longevity was fully suppressed by intestine-specific RNAi of all the downstream components, that is, *egl-30*/Gq, *egl-8*/PLCβ, *ckk-1*/CaMKK and *aak-2*/AMPK (Fig. 5a–d). This provides additional evidence that the octopamine receptor SER-3 regulates AMPK in the intestine via a Gq-PLCβ-CaMKK-dependent mechanism.

To obtain further evidence, we assessed whether the octopamine receptor SER-3 can promote AMPK activity, and if so, whether it acts in a Gq-PLCβ-CaMKK-dependent manner. Transgenic expression of SER-3 in the intestine stimulated AAK-2 phosphorylation (Fig. 5e), demonstrating that intestinal SER-3 can promote the activity of AMPK. Importantly, this SER-3-dependent AAK-2 activation was abrogated in *egl-30*/Gq, *egl-8*/PLCβ and *ckk-1*/CaMKK mutant worms (Fig. 5f–h). This experiment provides biochemical evidence that the octopamine receptor SER-3 promotes AMPK activity in a Gq-PLCβ-CaMKK-dependent manner.

Activation of norepinephrine signaling in mouse primary cells regulates AMPK via a similar Gq-PLCβ-CaMKK-dependent mechanism. Octopamine is the invertebrate homolog of norepinephrine. We then wondered if norepinephrine signaling could regulate AMPK in mammalian cells via a similar Gq-PLCβ-CaMKK-dependent mechanism. In *C. elegans*, the intestine also fulfills many of the complex functions of mammalian fat and liver tissues[35]. We thus characterized mouse primary subcutaneous adipocytes and primary hepatocytes, both of which express the Gq-coupled α1A-adrenergic receptor[36,37]. Selective activation of α1A-adrenergic receptor with cirazoline stimulated AMPK phosphorylation in mouse primary subcutaneous adipocytes and primary hepatocytes (Fig. 6a,b), indicating that activation of norepinephrine signaling can promote AMPK activity in these primary cells. Importantly, this AMPK activation was blocked by inhibitors of Gq (YM254890), PLC (U73122 but not its inactive analog U73343) and CaMKK (STO-609) (Fig. 6c–h). These data suggest that activation of norepinephrine signaling in mouse primary cells can stimulate AMPK via a Gq-PLCβ-CaMKK-dependent mechanism.

Food odors and DR converge on AMPK to regulate longevity. One notable observation is that among all the genes characterized in this study, AMPK is unique in that it is the only one that, when mutated, blocked the effects from both DR and food odors. Namely, *aak-2*/AMPK mutants were completely insensitive to both DR and food odors (Fig. 4a). By contrast, although mutants of other genes in the olfactory circuit and the downstream octopamine signaling failed to respond to food odors, they remained sensitive to DR at least partially in the lifespan assay (Supplementary Table 1). This unique feature of AMPK suggests that food odors and DR may converge on AMPK to regulate lifespan. AMPK is an energy sensor sensitive to DR[3,33]. Specifically, DR leads to an increase in the AMP:ATP ratio, resulting in activation of AMPK[3,33]. Notably, AMPK is under dual regulation, as its activation also requires phosphorylation by AMPK kinases such as CaMKK[3,33], which we showed is regulated by octopamine signaling residing downstream of the olfactory circuit. Thus, AMPK may sit at a unique position to integrate signals from DR and food odors (Fig. 6i). To test this, we mutated the CKK-1/CaMKK phosphorylation site in AAK-2/AMPK from threonine to aspartic acid (that is, AAK-2(T181D)) to render it insensitive to CKK-1/CaMKK, thereby uncoupling it from food odors. This AAK-2(T181D) is functional, as it rescued the DR longevity defect in *aak-2* mutant worms (Fig. 4i). Remarkably, worms expressing AAK-2(T181D) were insensitive to food odors (Fig. 4i), indicating that this mutant form of AAK-2/AMPK lost the ability to integrate signals from DR and food odors. This provides further evidence that food odors and DR converge on AAK-2/AMPK to regulate longevity.

Discussion

In the current study, we investigated how food-associated odors regulate DR longevity in *C. elegans*. The fact that food odors suppress the lifespan of worms under DR but not those fed AL highlights the notion that, in addition to the actual food abundance (nutrient level), the perception of food abundance (from food odors) is also important for longevity[5]. Our results suggest a model that food odors suppress DR longevity by acting on an olfactory circuit, which signals the gut intestine via octopamine, the invertebrate homology of norepinephrine, to regulate the energy sensor AMPK through a Gq-PLCβ-CaMKK-dependent mechanism (Fig. 6i). Interestingly, norepinephrine signaling can also regulate AMPK through a similar mechanism in mouse primary cells. These results identify a brain–gut axis through which food odors suppress DR-mediated longevity, illustrating how non-nutrient food components may regulate lifespan by altering animals' perception of food abundance.

The olfactory circuit comprises three pairs of neurons: ADF, CEP and RIC. In this circuit, food odors stimulate ADF to inhibit RIC via CEP (Fig. 6i). We also characterized the molecular mechanisms by which the circuit senses and processes odor signals by identifying some of the key components mediating sensory transduction and sensory processing (Fig. 6i). While CEP neurons form direct connections with RIC neurons, no such connections are found between ADF and CEP neurons[14], suggesting that part of this circuit is neuroendocrine by nature. We thus do not exclude the possibility that other neurons or cells may also be part of this circuit. For example, some other chemosensory neurons have also been suggested to modulate longevity[6,12,38]; however, whether these neurons can directly sense food odors to regulate lifespan remains to be determined. One interesting observation is that food odors elicited robust calcium responses in ADF, CEP and RIC neurons from DR worms, but not in those fed AL, revealing a DR-specific effect. It is possible that DR sensitized the neurons in the circuit. Alternatively, but not mutually exclusively, AL feeding may suppress the circuit responsiveness. In humans, fasting potentiates olfactory sensitivity, while satiety suppresses it[39], unveiling an interesting similarity between worms and mammals. Future studies will determine how DR and AL feeding differentially regulate the sensitivity of the olfactory system to food odors.

AMPK sits at a unique position to integrate signals from both food odors and DR due to its dual-regulation mode by AMP:ATP

ratio (DR) and CaMKK (food odors). AMPK primarily acts in the intestine to mediate this effect. Nevertheless, we do not exclude a role for AMPK in other tissues such as neurons, given that AMPK has the capacity to regulate lifespan in a non-cell-autonomous manner[40]. AMPK is probably not the only substrate regulated by both DR and food odors. For example, DR also regulates the sensitivity of the olfactory circuit to food odors. Nonetheless, our results suggest that AMPK is a primary site where food odors and DR converge to regulate longevity. Then, what acts downstream of AMPK? One downstream effector of AMPK is the transcription factor DAF-16/FOXO[10], which is a master regulator of longevity. AMPK regulates DAF-16/FOXO via direct phosphorylation[10,41]. We found that AAK-2/AMPK-dependent lifespan extension requires DAF-16 (Extended Data Fig. 6a), and that AAK-2/AMPK expression in the intestine promoted the expression of the DAF-16/FOXO target gene *sod-3* in a DAF-16-dependent manner (Extended Data Fig. 6b–d). SOD-3 expression was upregulated in a non-cell-autonomous manner in many other tissues, indicating that the longevity signal was disseminated throughout the body (Extended Data Fig. 6c), consistent with the notion that the intestine is a signaling hub for longevity regulation[1]. Another effector of AMPK could be mitochondria, as AMPK regulates mitochondrial function and dynamics to modulate longevity[42]. Thus, it is likely that multiple AMPK effectors may act downstream to regulate DR longevity.

We identify octopamine as a signaling molecule that mediates brain–gut communications. Specifically, our data suggest that food odors suppress octopamine signaling in the intestine by inhibiting octopamine release from the olfactory circuit. We also show that octopamine signaling regulates AMPK in the intestine via a Gq-PLCβ-CaMKK-dependent mechanism. Octopamine is the invertebrate homolog of norepinephrine. Remarkably, activation of norepinephrine signaling in mouse primary cells can stimulate AMPK in a similar manner, suggesting a conserved mechanism. Interestingly, blocking olfactory sensation in mice stimulates norepinephrine release from sympathetic nerves and promotes norepinephrine signaling in fat tissues, leading to improved energy metabolism and protection against obesity[43]. Conversely, enhancing olfaction in mice causes insulin resistance and obesity[43]. This raises the intriguing possibility that olfaction might inhibit longevity in mice through norepinephrine signaling, pointing to another potential similarity between worms and mice. It would be interesting to test whether those olfaction-deficient mice are long-lived.

Methods

Strains. *C. elegans* strains were maintained at 20 °C on NGM plates seeded with OP50 bacteria unless otherwise specified. Transgenic lines were generated by injecting plasmid DNA directly into the hermaphrodite gonad following standard protocol. Mutant strains were outcrossed at least six times before use. For genetic crosses, all genotypes were confirmed using PCR and, if necessary, followed by Sanger sequencing to verify single-nucleotide mutations. The strains used were:

- TQ3030 N2 (WT)
- TQ4931 *tph-1(mg280) II*
- TQ4935 *cat-2(e1112) II*
- TQ4927 *tbh-1(n3247) X*
- TQ4929 *tdc-1(n3419) II*
- TQ4933 *eat-4(ky5) III*
- TQ6452 *unc-17(e245) IV*
- TQ4168 *unc-25(e156) III*
- TQ1280 *unc-31(e169) IV*
- TQ9677 *xuEx255a[Ptph-1(L)::GCaMP6f + Ptph-1(L)::mcherry2]*
- TQ9984 *xuEx3388[Pdat-1::myr-GCaMP6f + Pdat-1::mcherry2]*
- TQ10132 *xuEx3312[Ptbh-1::GCaMP6f + Ptbh-1::mcherry2]*
- TQ10049 *xuEx255a[Ptph-1(L)::GCaMP6f + Ptph-1(L)::mcherrry2]; unc-13(e51) I*
- TQ10046 *xuEx255a[Ptph-1(L)::GCaMP6f + Ptph-1(L)::mcherry2]; unc-31(e169) IV*
- TQ10047 *xuEx255a[Ptph-1(L)::GCaMP6f + Ptph-1(L)::mcherry2]; cat-2(e1112) II*
- TQ10042 *xuEx255a[Ptph-1(L)::GCaMP6f + Ptph-1(L)::mcherry2]; tbh-1(n3247) X*
- TQ10003 *xuEx3388[Pdat-1::myr-GCaMP6f + Pdat-1::mcherry2]; tph-1(mg280) II*
- TQ10011 *xuEx3388[Pdat-1::myr-GCaMP6f + Pdat-1::mcherry2]; xuEx54a[Pbas-1(prom7)::TeTx::sl2::mcherry2 + Punc-122delta::gfp]*
- TQ10045 *xuEx3388[Pdat-1::myr-GCaMP6f + Pdat-1::mcherry2]; tbh-1(n3247) X*
- TQ9923 *xuEx3312[Ptbh-1::GCaMP6f + Ptbh-1::mcherry2]; tph-1(mg280) II*
- TQ10012 *xuEx3312[Ptbh-1::GCaMP6f + Ptbh-1::mcherry2]; xuEx54a[Pbas-1(prom7)::TeTx::sl2::mcherry2 + Punc-122delta::gfp]*
- TQ9858 *xuEx3312[Ptbh-1::GCaMP6f + Ptbh-1::mcherry2]; cat-2(e1112) II*
- TQ9939 *xuEx3312[Ptbh-1::GCaMP6f + Ptbh-1::mcherry2]; xuEx201a[Pdat-1::TeTx::sl2::mcherry2]*
- TQ9573 *xuEx54a[Pbas-1(prom7)::TeTx::sl2::mcherry2 + Punc-122delta::gfp]*
- TQ9571 *xuEx201a[Pdat-1::TeTx::sl2::mcherry2]*
- TQ9570 *xuEx197a[Ptbh-1::TeTx::sl2::mcherry2]*
- TQ600 *odr-3(n2150) V*
- TQ5663 *ocr-2(ak47) IV*
- TQ9883 *xuEx255a[Ptph-1(L)::GCaMP6f + Ptph-1(L)::mcherry2]; odr-3(n2150) V*
- TQ9860 *xuEx255a[Ptph-1(L)::GCaMP6f + Ptph-1(L)::mcherry2]; ocr-2(ak47) IV*
- TQ10107 *xuEx255a[Ptph-1(L)::GCaMP6f + Ptph-1(L)::mcherry2]; xuEx3402[Pbas-1(prom7)::odr-3(cDNA)::sl2::cfp]; odr-3(n2150) V*
- TQ10044 *xuEx255a[Ptph-1(L)::GCaMP6f + Ptph-1(L)::mcherry2]; xuEx3399[Pbas-1(prom7)::ocr-2(cDNA)::sl2::cfp]; ocr-2(ak47) IV*
- TQ9996 *xuEx3364[Pbas-1(prom7)::odr-3(cDNA)::sl2::yfp1]; odr-3(n2150) V*
- TQ9931 *xuEx3357[Pbas-1(prom7)::ocr-2(cDNA)::sl2::yfp1]; ocr-2(ak47) IV*
- TQ1615a *ser-5(ok3087) I*
- TQ9688 *xuEx191a[Pdat-1::ser-5(cDNA)::sl2::mcherry2]; ser-5(ok3087) I*
- TQ10005 *xuEx3388[Pdat-1::myr-GCaMP6f + Pdat-1::mcherry2]; ser-5(ok3087) I*
- TQ10025 *xuEx3388[Pdat-1::myr-GCaMP6f + Pdat-1::mcherry2]; xuEx3401[Pdat-1::ser-5(cDNA)::sl2::cfp]; ser-5(ok3087) I*
- TQ9820 *dop-6(n2090) X*
- TQ9932 *xuEx3312[Ptbh-1::GCaMP6f + Ptbh-1::mcherry2]; dop-6(ok2090) X*
- TQ10024 *xuEx3312[Ptbh-1::GCaMP6f + Ptbh-1::mcherry2]; xuEx3400[Ptbh-1::dop-6(cDNA)::sl2::cfp]; dop-6(ok2090) X*
- TQ9449 *xuEx3222[Ptbh-1::dop-6(cDNA)::sl2::yfp1]; dop-6(ok2090) X*
- TQ6682 *aak-2(ok524) X*
- TQ6511 *xuEx2334[Pges-1::aak-2(cDNA)::sl2::mcherry2]; aak-2(ok524) X*
- TQ1809a *sid-1(qt9) V*
- TQ9550 *xuEx3239[Pges-1::DsRed + Pges-1::aak-2(RNAi, s + as)]; sid-1(qt9) V*
- TQ9779 *ser-3(ok1995) I*
- TQ9503 *xuEx235a[Pges-1::ser-3(cDNA)::sl2::yfp1]; ser-3(ok1995) I*
- TQ9770 *xuEX3307[Pges-1::DsRed + Pges-1::ser-3(RNAi,s + as)]; sid-1(qt9) V*
- TQ9557 *xuEx3229[Pges-1::DsRed + Pges-1::egl-30(RNAi,s + as)]; sid-1(qt9) V*
- TQ9555 *xuEx3227[Pges-1::DsRed + Pges-1::egl-8(RNAi,s + as)]; sid-1(qt9) V*
- TQ9551 *xuEx3223[Pges-1::DsRed + Pges-1::ckk-1(RNAi,s + as)]; sid-1(qt9) V*
- TQ9548 *xuEx235a[Pges-1::ser-3(cDNA)::sl2::yfp1]; sid-1(qt9) V*
- TQ9458 *xuEx235a[Pges-1::ser-3(cDNA)::SL2::yfp1]; xuEx3229[Pges-1::DsRed + Pges-1::egl-30(RNAi,s + as)]; sid-1(qt9) V*
- TQ9456 *xuEx235a[Pges-1::ser-3(cDNA)::SL2::yfp1]; xuEx3227[Pges-1::DsRed + Pges-1::egl-8(RNAi,s + as)]; sid-1(qt9) V*
- TQ9452 *xuEx235a[Pges-1::ser-3(cDNA)::SL2::yfp1]; xuEx3223[Pges-1::DsRed + Pges-1::ckk-1(RNAi,s + as)]; sid-1(qt9) V*
- TQ9581 *xuEx235a[Pges-1::ser-3(cDNA)::sl2::yfp1]; xuEx3239[Pges-1::DsRed + Pges-1::aak-2(RNAi, s + as)]; sid-1(qt9) V*
- TQ9505 *xuEx3232[Pges-1::aak-2(T181D)::sl2::mcherry2]; aak-2(ok524) X*
- TQ3114a *xuEx235a[Pges-1::ser-3::sl2::yfp1]; egl-30(ep271) I*
- TQ3115a *xuEx235a[Pges-1::ser-3::sl2::yfp1]; egl-8(n488) V*
- TQ3116a *xuEx235a[Pges-1::ser-3::sl2::yfp1]; ckk-1(ok1033) III*

Chemical reagents. Collagenase D (11088882001) and dispase II (04942078001) were purchased from Roche. All the cell culture media, including DMEM (11995-073), low glucose DMEM (11885-084) and DMEM/F12 GlutaMAX (10565-042), were obtained from Life Technologies. Erioglaucine disodium salt (861146), 5-fluoro-2′-deoxyuridine (FUDR; F0503), 3-isobutyl-1-methylxanthine (IBMX; I7018), dexamethasone (D4902), insulin (I5500) and fetal bovine serum (FBS; F2442) were acquired from Sigma-Aldrich. Cirazoline hydrochloride (0888) and AICAR (2840) were purchased from Tocris. STO-609 (15325) and rosiglitazone (71740) were purchased from Cayman Chemical. YM2548909 (257-00631) was purchased from FUJIFILM Wako Chemicals. Collagenase type IV (LS004188) was obtained from Worthington Biochemical.

Mice. Animal care and experimental protocols were reviewed and approved by the Institutional Animal Care and Use Committee at the University of Michigan. Wild-type C57BL/6J mice (stock no. 00664) were obtained from the Jackson Laboratory and housed under a 12-h light/12-h dark cycle with a standard rodent chow diet (5L0D, PicoLab).

Molecular biology. The following promoters were used to drive gene expression in specific neurons and tissues: *tph-1(L)* promoter (2.1-kb 5′ UTR and 0.5-kb coding region) in serotonin neurons, including both ADF and NSM; *tph-1(s)* promoter (1.7 kb) in NSM neurons; *bas-1(prom7)* promoter (166 bp) in ADF neurons; *cex-1* promoter (1.1 kb) in RIM neurons[44]; *dat-1* promoter (0.8 kb) in CEP, ADE and PDE neurons; *tbh-1* promoter (4.4 kb) in RIC neurons; *rgef-1* promoter (3.4 kb) in all neurons; and *ges-1* promoter (3.2 kb) in the intestine. *odr-3*, *ocr-2*, *ser-5*, *dop-6*, *ser-3*, *egl-30*, *egl-8*, *ckk-1* and *aak-2* cDNA were cloned by RT–PCR from total RNA isolated from wild-type (N2) worms. To generate dsRNA plasmids, *ser-3*, *egl-30*, *egl-8*, *ckk-1*, *aak-2*, *par-4* and *mom-4* fragments were amplified from genomic DNA extracted from wild-type worms. The first 12 amino acids from NCS-2 protein were fused with GCaMP6f to make myr-GCaMP6f, a membrane-targeting form of GCaMP6f. The *dat-1* promoter was used to drive myr-GCaMP6f and DsRed expression in CEP neurons to facilitate imaging of the dendritic compartments of these neurons. To make tdTomato-expressing OP50 bacteria, tdTomato coding sequence was cloned into *pGEX-5x-3* vector and transformed into OP50 component cells.

Lifespan assays. Lifespan experiments were performed on NGM plates seeded with OP50 at 20°C. In all experiments, the first day of adulthood was scored as day 1. Worms that crawled off the plate, exploded or bagged were censored. DR lifespan assays (sDR) were performed as described in previous literature[45]. All assays were conducted on OP50. To harvest bacterial food, fresh OP50 colonies were inoculated in LB medium overnight (14–16 h), and bacteria pellets were collected by high-speed centrifugation (4,000 r.p.m. at 4 °C for 20 min). Bacteria pellets were resuspended in 10 ml fresh LB medium and pelleted again by centrifugation, and this step was repeated one more time. Lastly, bacteria pellets were resuspended in fresh LB medium containing 5 mg ml^{-1} carbenicillin to a final concentration of 10^{11} colony-forming units (c.f.u.) ml^{-1}. AL plates were prepared with a bacteria concentration of 10^{11} c.f.u. ml^{-1} (200 µl per plate), and DR plates with a bacteria concentration of 10^{9} c.f.u. ml^{-1} (200 µl per plate). FUDR was added to NGM plates at a final concentration of 2.5 µg ml^{-1} to prevent egg laying and bagging. Unless indicated otherwise, about 80–100 worms were transferred onto AL and DR plates at day 4 and then transferred every 2–4 d to fresh AL or DR NGM plates at a density of 15 worms per plate until day 19–20 for DR and day 15–16 for AL conditions. For lifespan assays under normal conditions, about 80–100 worms of each strain were included and transferred every 2–4 d until day 11–12 as described previously[46]. All statistical analyses were performed using Prism 6 (GraphPad) and SPSS Statistics 21 (IBM). *P* values were calculated using the log-rank (Kaplan–Meier) method.

Feeding and food ingestion measurements. To quantify feeding rate, day 4 adult worms were transferred to NGM plates seeded with DR or 2 × DR amount of bacterial food and randomly divided into two groups, with one group exposed to food odors and the other group not. Pharyngeal pumping rate was then counted under a stereoscope at 1 h, 24 h and 96 h after worms were transferred to DR plates at 20 °C.

To quantify food ingestion, OP50-tdTomato bacteria were used as food. Worms were transferred to NGM plates seeded with DR or 2 × DR amount of bacterial food and randomly divided into two groups, with one group exposed to food-derived odors and the other group not. At 1 h after transfer, worms were immobilized in 20 mM sodium azide/M13 solution, mounted on 2% agarose pads and imaged on an Olympus IX73 inverted microscope under a ×10 objective using ORCA-Flash4.0 LT+ digital CMOS camera (Hamamatsu) with MetaMorph software (Molecular Devices). ImageJ was used to quantify the images.

Calcium imaging. A microfluidic system was used to perform calcium imaging as previously described[47]. One to two days after transferring onto AL or DR plates, worms were loaded onto a microfluidic device mounted on an Olympus IX73 inverted microscope and incubated in M13 solution (30 mM Tris-Cl, 100 mM NaCl and 10 mM KCl; pH 7.0). Images were acquired under a ×40 objective using an ORCA-Flash4.0 LT+ digital CMOS camera (Hamamatsu) with MetaFluor software (Molecular Devices) at 1 Hz. GCaMP6f and DsRed were coexpressed as a transgene in specific neurons using corresponding promoters to enable ratiometric imaging under blue (484 nm) and yellow (565 nm) light. As food odor-evoked calcium responses are similar in different subcompartments in ADF and RIC neurons, we focused on recording soma signals in these two neurons. For CEP neurons, we focused on recording dendritic signals. This is because only dendritic responses in CEP neurons are DR dependent, while soma and axon responses do not depend on DR or the input from the upstream ADF neurons, indicating that CEP soma and axon responses are irrelevant to the DR pathway. We expressed myr-GCaMP6f in CEP neurons to facilitate dendritic imaging. Worms were first exposed to blue-yellow light cycles for 2 min in LB medium to establish a basal line before being challenged with LB medium containing food odors. To prepare LB medium containing food odors, OP50 bacteria were cultured in LB medium overnight (14–16 h), and the medium was collected by two rounds of high-speed centrifugation (each at 4,000 r.p.m. at 4 °C for 20 min) to remove all bacteria, followed by filtering through a 0.45-µm filter. Such medium was freshly prepared each time for the imaging experiment. Background fluorescence was subtracted when calculating the ratio of GCaMP:DsRed. The peak fold change in the ratio of GCaMP:DsRed fluorescence was analyzed.

Mouse primary cell isolation and culture. To prepare mouse primary subcutaneous adipocytes, the stromal vascular fraction (SVF) was first isolated from inguinal adipose tissues of C57BL/6J mice (aged 6–8 weeks; male and female) cultured and differentiated as described previously[48]. Specifically, inguinal adipose tissues were dissected, washed in PBS, minced and digested in PBS containing collagenase D (1.5 U ml^{-1}), dispase II (2.4 U ml^{-1}) and 10 mM $CaCl_2$ for 20 min in a 37 °C water bath with agitation. Digestion reaction was terminated by addition of culture medium consisting of DMEM/F12 GlutaMAX supplemented with 10% FBS and 1% penicillin–streptomycin. Tissue suspension was passed through a 100-µm cell strainer and centrifuged at 300–500*g* for 5 min to pellet SVF cells. The cell pellet was resuspended in culture medium, filtered through a 40-µm cell strainer and centrifuged as above. Isolated SVF cells were plated onto a collagen-coated 10-cm cell culture dish and grown in culture medium. Adipogenesis was induced with culture medium supplemented with 0.5 µg ml^{-1} insulin, 5 µM dexamethasone, 1 µM rosiglitazone and 0.5 mM IBMX in confluent cells. After 2 d of induction, cells were maintained in culture medium containing 0.5 µg ml^{-1} insulin for 3 d. Differentiated adipocytes were stimulated with 100 µM cirazoline for varying time durations as indicated in the figure or with 500 µM AICAR (15 min). To test inhibitors, cells were pretreated with 25 µM YM254890, 5 µM U73122, 5 µM U73343 or 5 µM STO-609 for 30 min, followed by 100 µM cirazoline for 60 min before cells were harvested for immunoblotting.

Primary hepatocytes were isolated from C57BL/6J mice as previously reported[49]. Mice were anesthetized, and the liver was perfused via an inferior vena cava with washing buffer (HBSS buffer containing 0.5 mM EGTA and 25 mM HEPES, pH 7.4), followed by digestion medium (low glucose DMEM supplemented with 200 mg l^{-1} $CaCl_2$, 1% penicillin–streptomycin, 15 mM HEPES and 100 U ml^{-1} collagenase IV). The digested liver was excised, diced in digestion medium and filtered through a 70-µm cell strainer. Isolated hepatocytes were washed twice and plated onto collagen-coated culture plates with isolation medium (DMEM/F12 GlutaMAX supplemented with 10% FBS, 1% penicillin–streptomycin, 1 µM dexamethasone and 0.1 µM insulin) for 1 h. The medium was replaced with culture medium (low glucose DMEM containing 10% FBS, 1% penicillin–streptomycin, 0.1 µM dexamethasone and 1 nM insulin). After 3 h, hepatocytes were maintained in culture medium without FBS overnight until treatment with 100 µM cirazoline (varying time durations as indicated in Fig. 6) or 500 µM AICAR (15 min). To test inhibitors, hepatocytes were pretreated with 25 µM YM254890, 5 µM U73122, 5 µM U73343 or 5 µM STO-609 for 30 min, followed by 100 µM cirazoline for 15 min before cells were harvested for immunoblotting.

Immunoblotting. Mouse primary cells were lysed in ice-cold RIPA buffer (50 mM Tris-HCl (pH 7.5), 1% Triton X-100, 1% sodium deoxycholate, 0.1% SDS, 150 mM NaCl and 1 mM phenylmethylsulfonyl fluoride) supplemented with a protease inhibitor cocktail (Roche) and phosphatase inhibitors (10 mM sodium fluoride, 60 mM β-glycerolphosphate (pH 7.5), 2 mM sodium orthovanadate and 10 mM sodium pyrophosphate). Proteins were separated by SDS–PAGE and transferred to nitrocellulose membranes. The blots were probed with the following primary antibodies obtained from Cell Signaling Technology: phospho-AMPKα Thr 172 (2531), AMPKα (2532), GAPDH (5174) and HSP90 (4874).

Total proteins from ~120 day 1 adult worms grown on OP50 bacteria at 20°C were extracted with 120 µl RIPA lysis buffer supplemented with protease inhibitor cocktail (Roche) and phosphatase inhibitors (Sigma-Aldrich) by ultrasound sonication. The samples were then heated to 100°C for 10 min, followed by high-speed centrifugation (13,000 r.p.m. at 4 °C for 5 min). Proteins were separated by SDS–PAGE and transferred to nitrocellulose membranes, which were probed with the following primary antibodies obtained from Cell Signaling Technology: phospho-AMPKα Thr 172 (2531) and β-actin (4970). The phospho-AMPKα Thr 172 antibody recognizes the phosphorylated form of *C. elegans* AAK-2/AMPK[50]. As AMPKα (2532) antibody does not recognize *C. elegans* AAK-2/AMPK, we used β-actin as a control for protein loading.

Intestinal barrier function assay. Worms were cultured at 25 °C and were removed at different days from NGM plates and incubated for 3 h in M9 medium containing fresh *Escherichia coli* OP50 (optical density of 0.5–0.6) mixed with 5% FD&C blue no.1 dye (erioglaucine disodium salt; Sigma-Aldrich). Subsequently, worms were collected and washed with fresh M9 buffer for three times and transferred to fresh NGM plates with fresh OP50 bacteria. Next, worms were immobilized on an agarose pad with 5 mM sodium azide, and images were acquired on an Olympus upright microscope with a digital camera (Canon). We quantified the percentage of worms with body-cavity leakage, characterized by the presence of dye outside the intestine.

Statistics and reproducibility. Samples were randomized and treated under the same conditions. The sample sizes were not predetermined with a statistical method, but they are similar to those reported previously[46,51,52]. The number of independent replicates is indicated in Supplementary Table 1 for lifespan assays. For other assays, experiments were repeated independently at least twice with similar results. Data collection and analysis were not performed blindly. We assumed data distribution to be normal, but did not test it formally. No data were excluded from the analysis. Quantification and statistical parameters are indicated in the figure legends or directly marked in the figures, including the statistical method, error bars, *n* numbers and *P* values. We applied one-way ANOVA, two-way ANOVA, student's *t*-test and log-rank test to determine statistical significance. Specifically, for those analyses involving multiple group comparisons, we applied one-way ANOVA followed by a post hoc test (Bonferroni). In the case of factor analysis (Fig. 4l), we applied two-way ANOVA followed by a post hoc test (Bonferroni). For those only involving two groups, we applied two-tailed student's *t*-test. Lifespan comparisons were calculated by log-rank test. *P* values less than 0.05 are considered statistically significant. One-way or two-way ANOVA tests were performed using Prism 8 (GraphPad). Two-tailed student's *t*-tests were performed using Excel (Microsoft). All lifespan analyses were performed using SPSS Statistics (IBM).

Reporting Summary. Further information on research design is available in the Nature Research Reporting Summary linked to this article.

Data availability

The datasets generated and analyzed during this study are either included within the manuscript or are available from the corresponding author on reasonable request.

Received: 1 July 2020; Accepted: 29 January 2021;
Published online: 15 March 2021

References

1. Kenyon, C. J. The genetics of ageing. *Nature* **464**, 504–512 (2010).
2. Fontana, L., Partridge, L. & Longo, V. D. Extending healthy life span—from yeast to humans. *Science* **328**, 321–326 (2010).
3. Greer, E. L., Banko, M. R. & Brunet, A. AMP-activated protein kinase and FoxO transcription factors in dietary restriction-induced longevity. *Ann. N. Y. Acad. Sci.* **1170**, 688–692 (2009).
4. Kapahi, P., Kaeberlein, M. & Hansen, M. Dietary restriction and life span: lessons from invertebrate models. *Ageing Res. Rev.* **39**, 3–14 (2017).
5. Gendron, C. M. et al. Neuronal mechanisms that drive organismal aging through the lens of perception. *Annu. Rev. Physiol.* **82**, 227–249 (2020).
6. Alcedo, J. & Kenyon, C. Regulation of *C. elegans* longevity by specific gustatory and olfactory neurons. *Neuron* **41**, 45–55 (2004).
7. Apfeld, J. & Kenyon, C. Regulation of life span by sensory perception in *Caenorhabditis elegans*. *Nature* **402**, 804–809 (1999).
8. Libert, S. et al. Regulation of *Drosophila* life span by olfaction and food-derived odors. *Science* **315**, 1133–1137 (2007).
9. Greer, E. L. & Brunet, A. Different dietary restriction regimens extend life span by both independent and overlapping genetic pathways in *C. elegans*. *Aging Cell* **8**, 113–127 (2009).
10. Greer, E. L. et al. An AMPK–FOXO pathway mediates longevity induced by a novel method of dietary restriction in *C. elegans*. *Curr. Biol.* **17**, 1646–1656 (2007).
11. Smith, E. D. et al. Age- and calorie-independent life span extension from dietary restriction by bacterial deprivation in *Caenorhabditis elegans*. *BMC Dev. Biol.* **8**, 49 (2008).
12. Artan, M. et al. Food-derived sensory cues modulate longevity via distinct neuroendocrine insulin-like peptides. *Genes Dev.* **30**, 1047–1057 (2016).
13. Bargmann, C. I. Chemosensation in *C. elegans*. *WormBook* **25**, 1–29 (2006).
14. White, J. G., Southgate, E., Thomson, J. N. & Brenner, S. The structure of the nervous system of the nematode *Caenorhabditis elegans*. *Philos. Trans. R. Soc. Lond. B Biol. Sci.* **314**, 1–340 (1986).
15. Kang, L., Gao, J., Schafer, W. R., Xie, Z. & Xu, X. Z. S. *C. elegans* TRP family protein TRP-4 is a pore-forming subunit of a native mechanotransduction channel. *Neuron* **67**, 381–391 (2010).
16. Sawin, E. R., Ranganathan, R. & Horvitz, H. R. *C. elegans* locomotory rate is modulated by the environment through a dopaminergic pathway and by experience through a serotonergic pathway. *Neuron* **26**, 619–631 (2000).
17. Li, W., Feng, Z., Sternberg, P. W. & Xu, X. Z. S. A *C. elegans* stretch receptor neuron revealed by a mechanosensitive TRP channel homologue. *Nature* **440**, 684–687 (2006).
18. Alkema, M. J., Hunter-Ensor, M., Ringstad, N. & Horvitz, H. R. Tyramine functions independently of octopamine in the *Caenorhabditis elegans* nervous system. *Neuron* **46**, 247–260 (2005).
19. Shao, J. et al. Serotonergic neuron ADF modulates avoidance behaviors by inhibiting sensory neurons in *C. elegans*. *Pflugers Arch.* **471**, 357–363 (2019).
20. Richmond, J. E., Davis, W. S. & Jorgensen, E. M. UNC-13 is required for synaptic vesicle fusion in *C. elegans*. *Nat. Neurosci.* **2**, 959–964 (1999).
21. Speese, S. et al. UNC-31 (CAPS) is required for dense-core vesicle but not synaptic vesicle exocytosis in *Caenorhabditis elegans*. *J. Neurosci.* **27**, 6150–6162 (2007).
22. Link, E. et al. Tetanus toxin action: inhibition of neurotransmitter release linked to synaptobrevin proteolysis. *Biochem. Biophys. Res. Commun.* **189**, 1017–1023 (1992).
23. Hendricks, M., Ha, H., Maffey, N. & Zhang, Y. Compartmentalized calcium dynamics in a *C. elegans* interneuron encode head movement. *Nature* **487**, 99–103 (2012).
24. Li, Z., Liu, J., Zheng, M. & Xu, X. Z. Encoding of both analog- and digital-like behavioral outputs by one *C. elegans* interneuron. *Cell* **159**, 751–765 (2014).
25. Sokolchik, I., Tanabe, T., Baldi, P. F. & Sze, J. Y. Polymodal sensory function of the *Caenorhabditis elegans* OCR-2 channel arises from distinct intrinsic determinants within the protein and is selectively conserved in mammalian TRPV proteins. *J. Neurosci.* **25**, 1015–1023 (2005).
26. Hobert, O. in *WormBook* (Ed. The *C. elegans* Research Community) 1–106 (WormBook, 2013).
27. Blackwell, T. K., Sewell, A. K., Wu, Z. & Han, M. TOR signaling in *Caenorhabditis elegans* development, metabolism and aging. *Genetics* **213**, 329–360 (2019).
28. Winston, W. M., Molodowitch, C. & Hunter, C. P. Systemic RNAi in C. elegans requires the putative transmembrane protein SID-1. *Science* **295**, 2456–2459 (2002).
29. Rera, M., Clark, R. I. & Walker, D. W. Intestinal barrier dysfunction links metabolic and inflammatory markers of aging to death in *Drosophila*. *Proc. Natl Acad. Sci. USA* **109**, 21528–21533 (2012).
30. Gelino, S. et al. Intestinal autophagy improves healthspan and longevity in *C. elegans* during dietary Restriction. *PLoS Genet.* **12**, e1006135 (2016).
31. Dambroise, E. et al. Two phases of aging separated by the Smurf transition as a public path to death. *Sci. Rep.* **6**, 23523 (2016).
32. Yoshida, M., Oami, E., Wang, M., Ishiura, S. & Suo, S. Nonredundant function of two highly homologous octopamine receptors in food-deprivation-mediated signaling in *Caenorhabditis elegans*. *J. Neurosci. Res.* **92**, 671–678 (2014).
33. Burkewitz, K., Zhang, Y. & Mair, W. B. AMPK at the nexus of energetics and aging. *Cell Metab.* **20**, 10–25 (2014).
34. Neves, S. R., Ram, P. T. & Iyengar, R. G protein pathways. *Science* **296**, 1636–1639 (2002).
35. Dimov, I. & Maduro, M. F. The *C. elegans* intestine: organogenesis, digestion and physiology. *Cell Tissue Res.* **377**, 383–396 (2019).
36. Lafontan, M. & Berlan, M. Fat cell adrenergic receptors and the control of white and brown fat cell function. *J. Lipid Res.* **34**, 1057–1091 (1993).
37. Graham, R. M., Perez, D. M., Hwa, J. & Piascik, M. T. alpha 1-adrenergic receptor subtypes. Molecular structure, function and signaling. *Circ. Res.* **78**, 737–749 (1996).
38. Finger, F. et al. Olfaction regulates organismal proteostasis and longevity via microRNA-dependent signalling. *Nat. Metab.* **1**, 350–359 (2019).
39. Albrecht, J. et al. Olfactory detection thresholds and pleasantness of a food-related and a non-food odour in hunger and satiety. *Rhinology* **47**, 160–165 (2009).
40. Burkewitz, K. et al. Neuronal CRTC-1 governs systemic mitochondrial metabolism and life span via a catecholamine signal. *Cell* **160**, 842–855 (2015).
41. Greer, E. L. et al. The energy sensor AMP-activated protein kinase directly regulates the mammalian FOXO3 transcription factor. *J. Biol. Chem.* **282**, 30107–30119 (2007).
42. Weir, H. J. et al. Dietary restriction and AMPK increase life span via mitochondrial network and peroxisome remodeling. *Cell Metab.* **26**, 884–896 (2017).
43. Riera, C. E. et al. The sense of smell impacts metabolic health and obesity. *Cell Metab.* **26**, 198–211 (2017).
44. Piggott, B. J., Liu, J., Feng, Z., Wescott, S. A. & Xu, X. Z. S. The neural circuits and synaptic mechanisms underlying motor initiation in *C. elegans*. *Cell* **147**, 922–933 (2011).

45. Ching, T. T. & Hsu, A. L. Solid plate-based dietary restriction in *Caenorhabditis elegans*. *J. Vis. Exp*. https://doi.org/10.3791/2701 (2011).
46. Zhang, B. et al. Brain–gut communications via distinct neuroendocrine signals bidirectionally regulate longevity in *C. elegans*. *Genes Dev.* **32**, 258–270 (2018).
47. Wang, X., Li, G., Liu, J., Liu, J. & Xu, X. Z. S. TMC-1 mediates alkaline sensation in *C. elegans* through nociceptive neurons. *Neuron* **91**, 146–154 (2016).
48. Jun, H. et al. An immune-beige adipocyte communication via nicotinic acetylcholine receptor signaling. *Nat. Med.* **24**, 814–822 (2018).
49. Qiao, X. et al. Protein arginine methyltransferase 1 interacts with pgc1α and modulates thermogenic fat activation. *Endocrinology* **160**, 2773–2786 (2019).
50. Hwang, A. B. et al. Feedback regulation via AMPK and HIF-1 mediates ROS-dependent longevity in *Caenorhabditis elegans*. *Proc. Natl Acad. Sci. USA* **111**, E4458–E4467 (2014).
51. Xiao, R. et al. A genetic program promotes *C. elegans* longevity at cold temperatures via a thermosensitive TRP channel. *Cell* **152**, 806–817 (2013).
52. Zhang, B. et al. Environmental temperature differentially modulates *C. elegans* longevity through a thermosensitive TRP channel. *Cell Rep.* **11**, 1414–1424 (2015).

Acknowledgements

We thank J. Gong, S. Zhang and H. Chen for assistance. Some strains were obtained from the Caenorhabditis Genetics Center. J.L. received funding support from the National Natural Science Foundation of China (81872945 and 81720108031). J.W. received funding support from the National Institute of Diabetes and Digestive and Kidney Diseases (R01DK107583). X.Z.S.X. received funding support from the National Institute of General Medical Sciences (R35GM126917).

Author contributions

B.Z. conducted the experiments and analyzed the data. H.J., B.Z. and J.W. performed mouse experiments and analyzed the data. B.Z., J.L. and X.Z.S.X. wrote the paper with assistance from other authors.

Competing interests

The authors declare no competing interests.

Additional information

Extended data is available for this paper at https://doi.org/10.1038/s43587-021-00039-1.

Supplementary information The online version contains supplementary material available at https://doi.org/10.1038/s43587-021-00039-1.

Correspondence and requests for materials should be addressed to J.L. or X.Z.S.X.

Peer review information *Nature Aging* thanks Andrew Dillin and the other, anonymous, reviewer(s) for their contribution to the peer review of this work.

Reprints and permissions information is available at www.nature.com/reprints.

Publisher's note Springer Nature remains neutral with regard to jurisdictional claims in published maps and institutional affiliations.

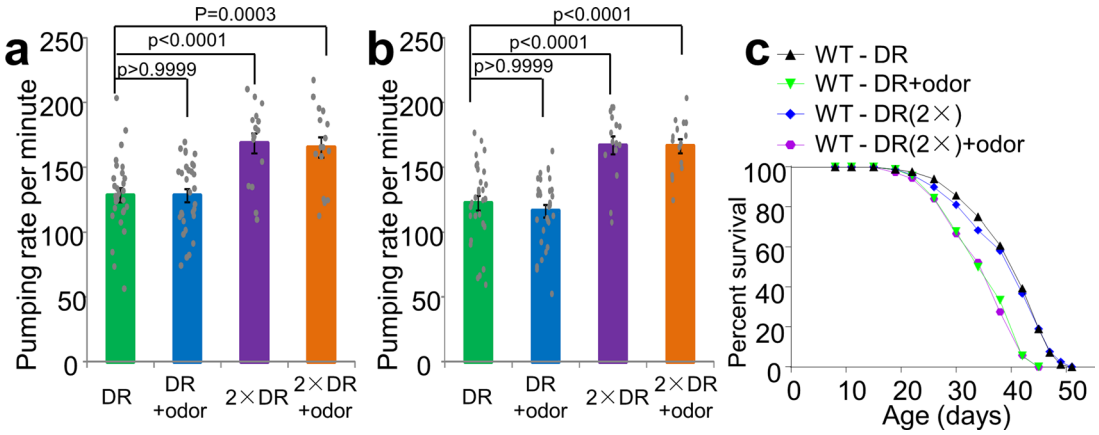

Extended Data Fig. 1 | Additional data related to food odor suppression of DR longevity without increasing food ingestion. a, b, Food odors do not change the pumping rate of worms under DR. Pumping rate was counted at 24 hr (**a**), and 96 hr (**b**), after worms were transferred to the DR assaying plates. 2×DR: twice amount of bacterial food, which stimulated the pumping rate. n = 30 (DR), 30 (DR + odor), 16 (2xDR) and 16 (2xDR + odor) biologically independent animals in (**a**). n = 30 (DR), 30 (DR + odor), 15 (2xDR) and 14 (2xDR + odor) biologically independent animals in (**b**). Data are presented as mean ± s.e.m. P values were calculated with one-way ANOVA with Bonfferroni's test. See Fig. 1c for data of the pumping rate counted at 1 hr post-transfer. **c**, Feeding worms with twice amount of bacteria food (2x DR) does not affect DR longevity, but food odors can still suppress the lifespan of these worms.

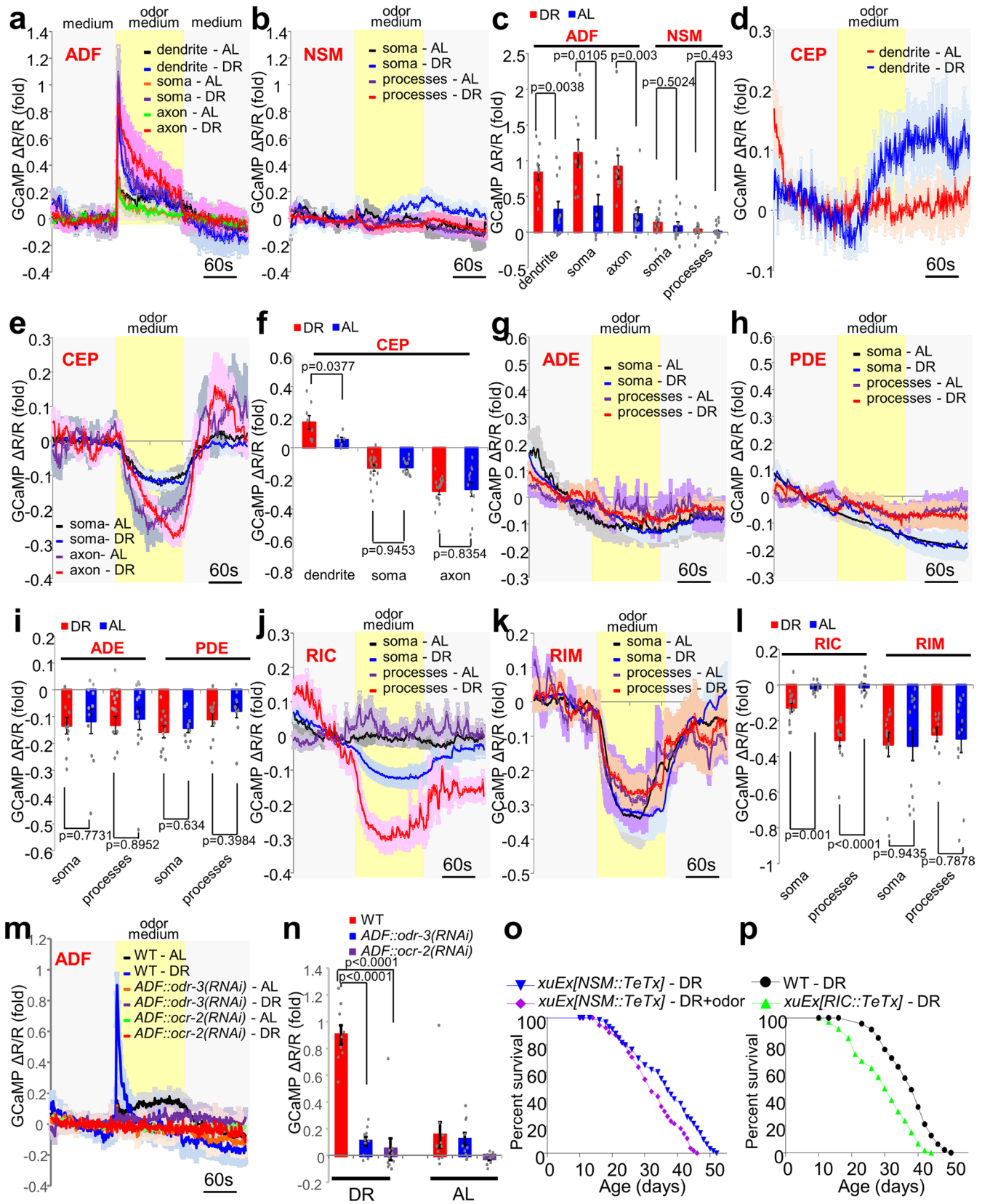

Extended Data Fig. 2 | See next page for caption.

Extended Data Fig. 2 | Additional data related to the olfactory circuit. a, ADF dendrite, soma and axon from DR, but not AL worms, all respond robustly to medium containing food odors. GCaMP6f was expressed as a transgene in ADF neurons under *tph-1(L)* promoter. DsRed was co-expressed to enable ratiometric imaging. Shades along the traces represent error bars (SEM). **b**, NSM neurons (dendrite/soma/axon) from DR and AL worms do not respond to medium containing food odors. GCaMP6f was expressed as a transgene in the NSM neurons using *tph-1(s)* promoter. DsRed was co-expressed to enable ratiometric imaging. Shades along the traces represent error bars (SEM). **c**, Bar graph summarizing data in (**a**) and (**b**). n = 11 (ADF dendrite - AL), 10 (ADF dendrite - DR), 8 (ADF soma - AL), 9 (ADF soma - DR), 11 (ADF axon - AL), 10 (ADF axon - DR), 11 (NSM soma - AL), 14 (NSM soma - DR), 13 (NSM processes - AL), and 10 (NSM processes - DR) biologically independent animals. **d**, CEP dendrite from DR worms, but not AL worms, responds robustly to medium containing food odors. GCaMP6f was expressed as a transgene in CEP neurons using *dat-1* promoter. DsRed was co-expressed to enable ratiometric imaging. Shades along the traces represent error bars (SEM). **e**, CEP soma and axon from both DR and AL worms respond to medium containing food odors, showing no specificity towards DR. Shades along the traces represent error bars (SEM). **f**, Bar graph summarizing data in (**d**) and (**e**). n = 6 (CEP dendrite - AL), 8 (CEP dendrite - DR), 13 (CEP soma - AL), 20 (CEP soma - DR), 12 (CEP axon - AL) and 17 (CEP axon - DR) biologically independent animals. **g, h**, ADE and PDE neurons (soma and processes) from DR and AL worms do not respond to medium containing food odors. GCaMP6f was expressed as a transgene in ADE and PDE neurons using *dat-1* promoter. DsRed was co-expressed to enable ratiometric imaging. Shades along the traces represent error bars (SEM). **i**, Bar graph summarizing data in (**g**) and (**h**). n = 11 (ADE soma - AL), 10 (ADE soma - DR), 13 (ADE processes - AL), 15 (ADE processes - DR), 10 (PDE soma - AL), 11 (PDE soma - DR), 10 (PDE processes - AL) and 11 (PDE processes - DR) biologically independent animals. **j**, RIC soma and processes from DR worms, but not AL worms, respond robustly to medium containing food odors. GCaMP6f was expressed as a transgene in RIC neurons under *tbh-1* promoter. DsRed was co-expressed to enable ratiometric imaging. Shades along the traces represent error bars (SEM). The soma traces are duplicates of those presented in Fig. 2i, as these experiments were performed at the same time. **k**, RIM soma and axon from both DR and AL worms respond to medium containing food odors, showing no specificity towards DR. GCaMP6f was expressed as a transgene in RIM neurons using *cex-1* promoter. DsRed was co-expressed to enable ratiometric imaging. Shades along the traces represent error bars (SEM). **l**, Bar graph summarizing data in (**j**) and (**k**). n = 11 (RIC soma - AL), 14 (RIC soma - DR), 11 (RIC processes - AL), 12 (RIC processes - DR), 12 (RIM soma - AL), 12 (RIM soma - DR), 12 (RIM processes - AL) and 10 (RIM processes - DR) biologically independent animals. **m, n,** RNAi knockdown of *odr-3* and *ocr-2* specifically in ADF neurons eliminates food odor-evoked calcium responses in these neurons. dsRNA against *odr-3* and *ocr-2* gene was expressed as a transgene specifically in ADF neurons using the *bas-1(prom7)* promoter. (**m**) Calcium imaging traces. Shades along the traces represent error bars (SEM). (**n**) Bar graph summarizing the data in (m). n = 10 (WT - AL), 9 (WT - DR), 10 (*ADF odr-3(RNAi)* - AL), 10 (*ADF odr-3(RNAi)* - DR), 10 (*ADF ocr-2(RNAi)* - AL) and 10 (*ADF ocr-2(RNAi)* - DR) biologically independent animals. (**o**) NSM neurons are not required for food odors to suppress DR longevity. *tph-1(s)* promoter was used to drive the expression of *TeTx* transgene specifically in NSM neurons. (**p**) Blocking the output of RIC neuron shortens DR longevity. *tbh-1* promoter was used to drive the expression of *TeTx* transgene in RIC neurons. Data are presented as mean ± s.e.m. P values in **c**, **f**, **i** and **l**: two-tailed student's t test. P values in **n**: one-way ANOVA with Bonfferroni's test.

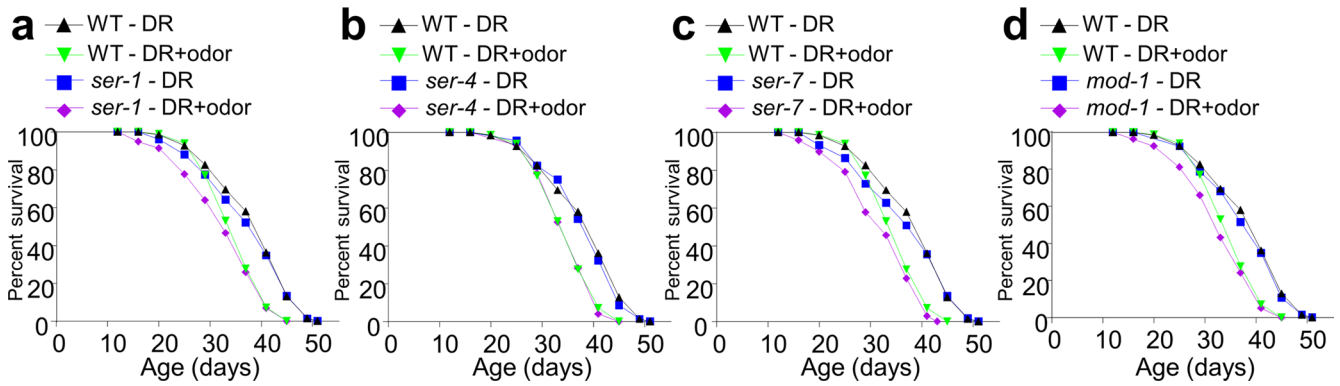

Extended Data Fig. 3 | Other serotonin receptors are not required for food odors to suppress DR longevity. Food odors can still suppress DR longevity in *ser-1* (**a**), *ser-4* (**b**), *ser-7* (**c**) and *mod-1* (**d**) mutant worms. **a-d**, share the same control group, as these experiments were performed at the same time.

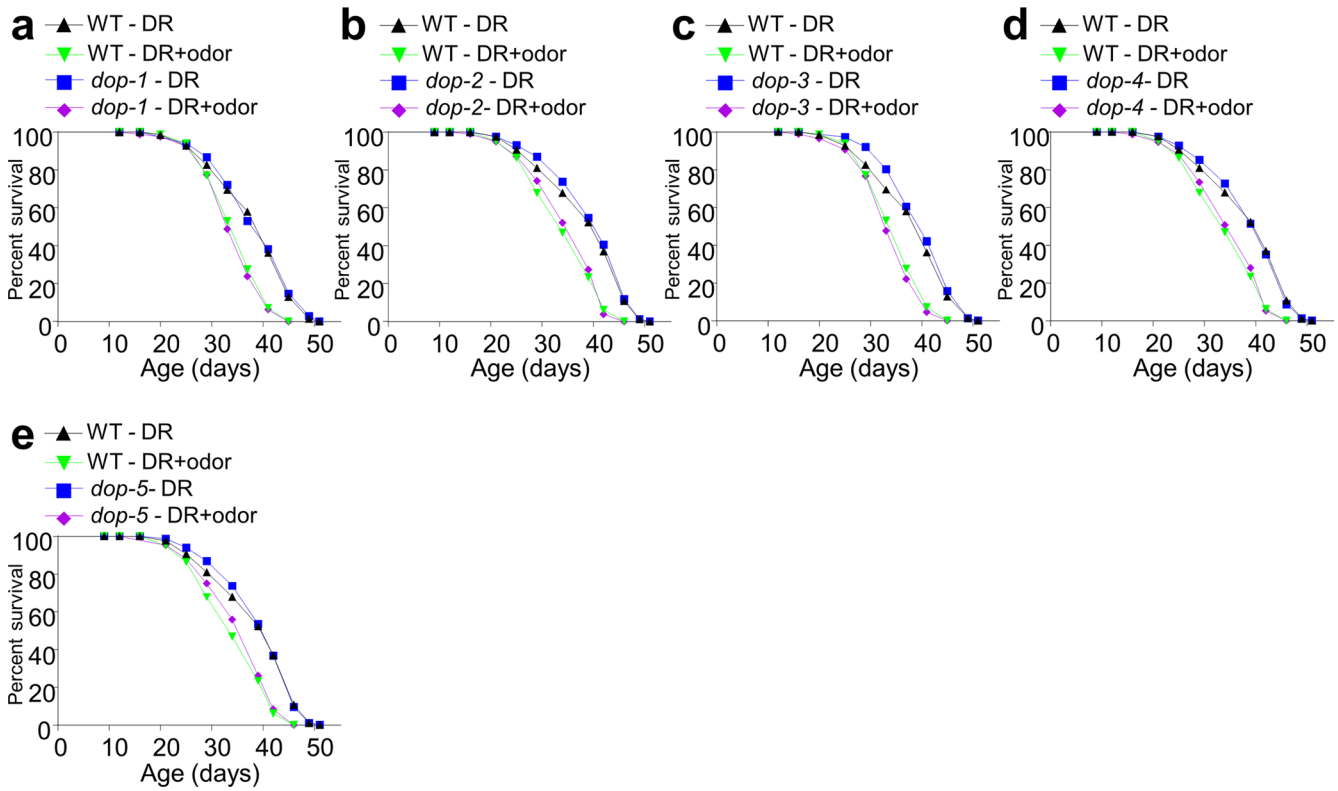

Extended Data Fig. 4 | Other dopamine receptors are not required for food odors to suppress DR longevity. Food odors can still suppress DR longevity in *dop-1* (**a**) *dop-2* (**b**) *dop-3* (**c**) *dop-4* (**d**) and *dop-5* (**e**) mutant worms. (**a**) and (**c**) share the same control group, as these experiments were performed at the same time. (**b**), (**d**) and (**e**) share the same control group, as these experiments were performed at the same time.

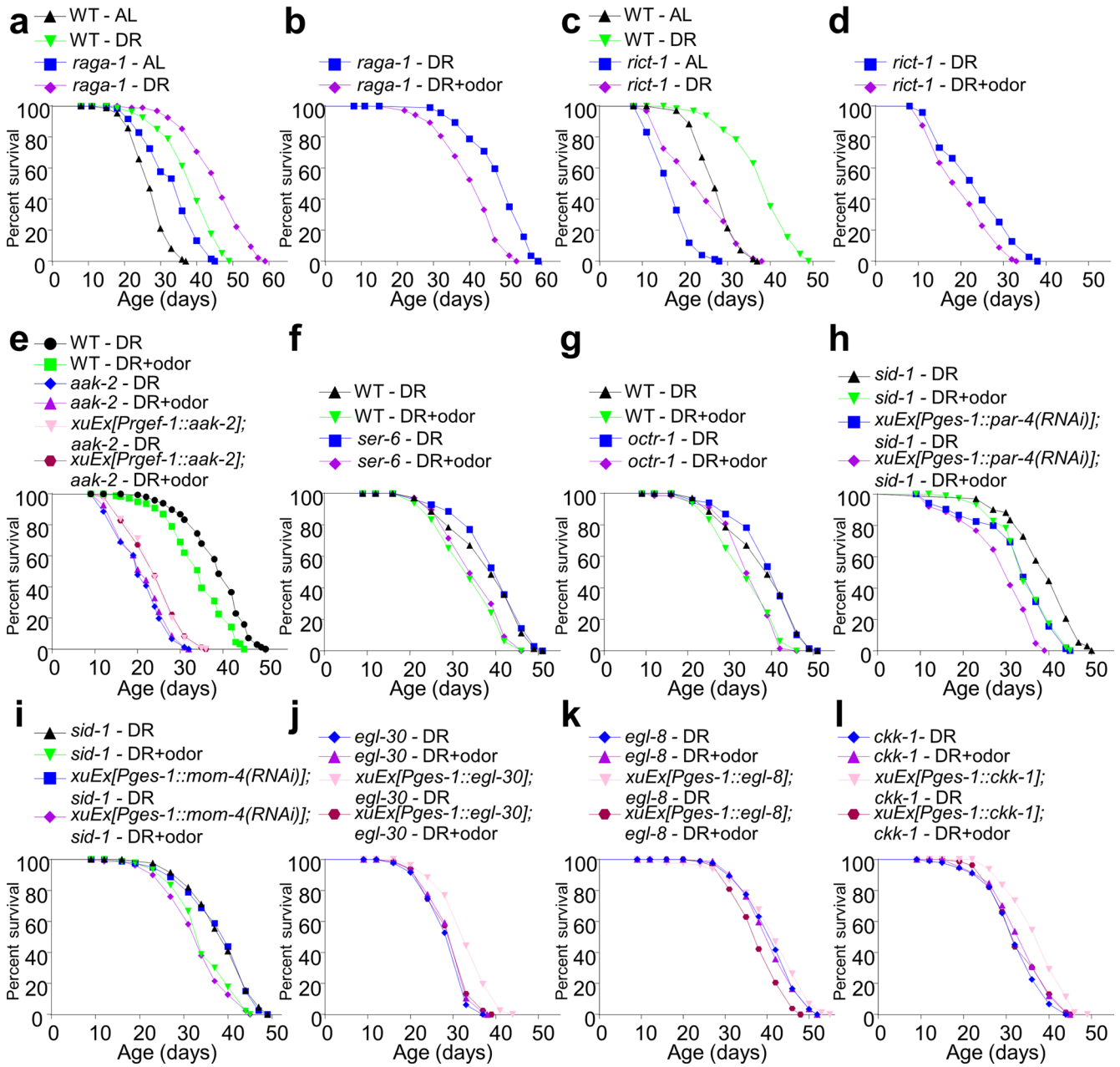

Extended Data Fig. 5 | Additional data related to regulation of DR longevity by AMPK and octopamine signaling. a, DR can extend the lifespan of *raga-1* mutant worms. **b**, Food odors can suppress DR longevity in *raga-1* mutant worms. **c**, DR can extend the lifespan of *rict-1* mutant worms. **d**, Food odors can suppress DR longevity in *rict-1* mutant worms. **e,** Pan-neuronal expression of *aak-2* gene only has a slight rescue effect on the longevity defect of *aak-2* mutant worms. This *aak-2* neuronal transgene also does not rescue the odor sensitivity defect of *aak-2* mutant worms. *rgef-1* promoter was used to drive the expression of *aak-2* cDNA in neurons. **f-g,** Food odors can still suppress DR longevity in *ser-6* (**f**) and *octr-1* (**g**) mutant worms. (**f**) and (**g**) share the same control group, as these experiments were performed at the same time. **h**, Intestine-specific knock-down of *par-4/LKB1* by dsRNA transgene *(Pges-1::par-4(RNAi))* does not prevent food odors from suppressing DR longevity, though it partially inhibits DR longevity. **i**, Intestine-specific knock-down of *mom-4/TAK1* by dsRNA transgene *(Pges-1::mom-4(RNAi))* does not prevent food odors from suppressing DR longevity; nor does it affect DR longevity. **j–l**, Mutations in *egl-30* (**j**), *egl-8* (**k**), and *ckk-1* (**l**) abolish the ability of food odors to suppress DR longevity, a defect that is rescued by transgenic expression of corresponding wild-type genes in the intestine using *ges-1* promoter.

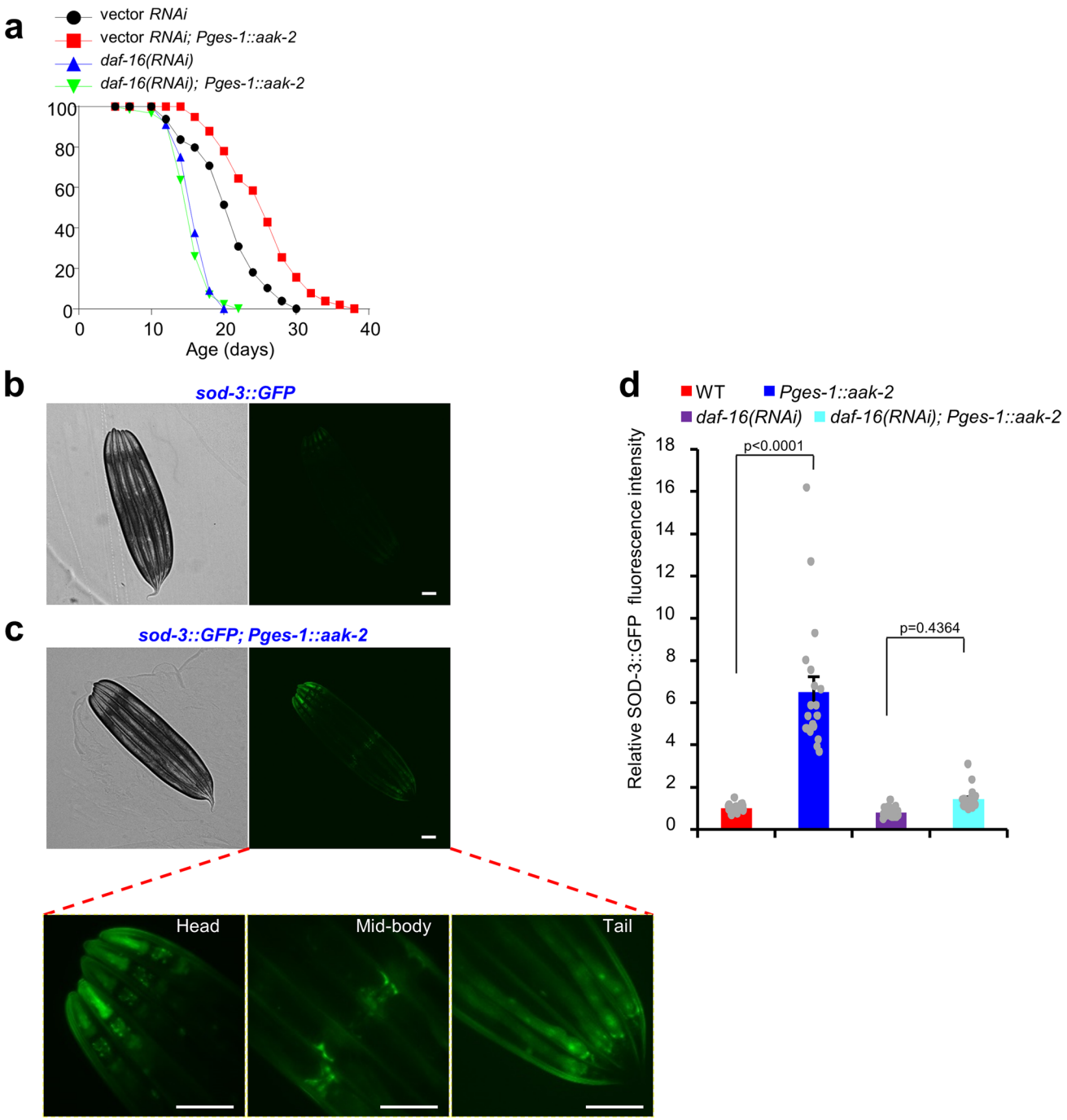

Extended Data Fig. 6 | AAK-2/AMPK-dependent lifespan extension requires DAF-16/FOXO. a, Lifespan extension mediated by intestinal expression of *aak-2* requires *daf-16*. *daf-16 RNAi* blocked the lifespan-extension effect of the intestinal *aak-2* transgene. **b-d**, Intestinal expression of *aak-2* promotes *sod-3* gene expression in multiple tissues in a *daf-16*-dependent manner. *sod-3::gfp* is a transgene reporting the expression level of *sod-3* gene. (**b**) Sample images showing a low level of *sod-3::gfp* expression. Left: bright field image. Right: fluorescent image. (**c**) Sample images showing that the *Pges-1::aak-2* transgene increased the expression of *sod-3::gfp*. Top left: bright field image. Top right: fluorescent image. Bottom: zoomed-in images showing *sod-3::gfp* expression in multiple tissues, including pharynx (head), neurons (head), body-wall muscles, vulval muscles (mid-body), intestine, etc. Scale Bar: 100 μm. (**d**) Bar graph summarizing the data in (**b**) and (**c**). n = 24 (WT), 20 (*Pges-1::aak-2*), 43 (*daf-16(RNAi)*) and 22 (*daf-16(RNAi); Pges-1::aak-2*) biologically independent animals. Data are presented as mean ± s.e.m. P values were calculated with one-way ANOVA with Bonfferroni's test.

nature research

Corresponding author(s): X.Z. Shawn Xu & Jianfeng Liu

Last updated by author(s): Jan 23, 2021

Reporting Summary

Nature Research wishes to improve the reproducibility of the work that we publish. This form provides structure for consistency and transparency in reporting. For further information on Nature Research policies, see our Editorial Policies and the Editorial Policy Checklist.

Statistics

For all statistical analyses, confirm that the following items are present in the figure legend, table legend, main text, or Methods section.

n/a	Confirmed	
☐	☒	The exact sample size (*n*) for each experimental group/condition, given as a discrete number and unit of measurement
☐	☒	A statement on whether measurements were taken from distinct samples or whether the same sample was measured repeatedly
☐	☒	The statistical test(s) used AND whether they are one- or two-sided *Only common tests should be described solely by name; describe more complex techniques in the Methods section.*
☐	☒	A description of all covariates tested
☐	☒	A description of any assumptions or corrections, such as tests of normality and adjustment for multiple comparisons
☐	☒	A full description of the statistical parameters including central tendency (e.g. means) or other basic estimates (e.g. regression coefficient) AND variation (e.g. standard deviation) or associated estimates of uncertainty (e.g. confidence intervals)
☐	☒	For null hypothesis testing, the test statistic (e.g. *F*, *t*, *r*) with confidence intervals, effect sizes, degrees of freedom and *P* value noted *Give P values as exact values whenever suitable.*
☒	☐	For Bayesian analysis, information on the choice of priors and Markov chain Monte Carlo settings
☒	☐	For hierarchical and complex designs, identification of the appropriate level for tests and full reporting of outcomes
☒	☐	Estimates of effect sizes (e.g. Cohen's *d*, Pearson's *r*), indicating how they were calculated

Our web collection on statistics for biologists contains articles on many of the points above.

Software and code

Policy information about availability of computer code

Data collection	All fluorescent images were acquired using the MetaMorph Image Analysis Software (Version 7.8.0.0, Molecular Devices). Ratiometric calcium imaging was performed with MetaFluor Fluorescence Ratio Imaging Software (Version 7.8.0.0, Molecular Devices)
Data analysis	Fluorescent image analysis and processing were performed using the ImageJ software. For lifespan assays, all statistical analyses were performed using GraphPad Prism 8 (GraphPad Software, Inc.) and IBM SPSS Statistics 21 (IBM, Inc.). Excel (Microsoft) was used to process ratiometric calcium imaging data points, and GraphPad Prism 8 (GraphPad Software, Inc.) was used to perform the statistic analyses for calcium imaging results. Image quantification for western blot was performed using ImageJ(version 1.52a) software. More details are provided in the methods section.

For manuscripts utilizing custom algorithms or software that are central to the research but not yet described in published literature, software must be made available to editors and reviewers. We strongly encourage code deposition in a community repository (e.g. GitHub). See the Nature Research guidelines for submitting code & software for further information.

Data

Policy information about availability of data

All manuscripts must include a data availability statement. This statement should provide the following information, where applicable:

- Accession codes, unique identifiers, or web links for publicly available datasets
- A list of figures that have associated raw data
- A description of any restrictions on data availability

All data generated or analyzed during this study are included in the figures and texts (and the supplementary information files). Further information can be requested from the corresponding author.

Field-specific reporting

Please select the one below that is the best fit for your research. If you are not sure, read the appropriate sections before making your selection.

☒ Life sciences ☐ Behavioural & social sciences ☐ Ecological, evolutionary & environmental sciences

For a reference copy of the document with all sections, see nature.com/documents/nr-reporting-summary-flat.pdf

Life sciences study design

All studies must disclose on these points even when the disclosure is negative.

Sample size	Samples sizes are described in Supplemental Table 1 or figure legends. No statistical methods were used to predetermine sample size. Our samples sizes for each experiment are based on prior knowledge and expertise and are typical of those used in the field. Specifically, For lifespan assays,about 80-100 worms were included for each group/treatment (Four glial cells regulate ER stress resistance and longevity via neuropeptide signaling in C. elegans, Science, 2020/NuRD mediates mitochondrial stress–induced longevity via chromatin remodeling in response to acetyl-CoA level, Science Advances, 2020). And, each sample for Western blotting are prepared with total proteins from ~120 Adult worms(C. elegans S6K Mutants Require a Creatine-Kinase-like Effector for Lifespan Extension, Cell Reports, 2016). Comparable sample sizes for each genotype/condition were used in every experiment
Data exclusions	No data points were excluded from our analyses.
Replication	For lifespan assays, every experiment was replicated at least twice using independent worms collected at different days with similar results. For other worm related experiments, at least 3 biological replicates were performed at different days, and similar results were collected. The rest experiments were repeated at least once with similar results.
Randomization	Experimental and control worms were maintained under the same conditions and allocated to treatments/groups randomly (for example, with regard to odor conditioning medium treatment, dietary restriction treatment, etc).
Blinding	For analyses related to worms, the genotypes of worms were not blinded to the experimenter. Given the genotypes of worms need to be carefully documented by the investigators, so blinding was not always possible during experimental setup. When possible, we randomly allocated worms with the same genotype from the same batch to different treatments and collected the results blindingly. In addition, control and experimental worms/samples were treated equally and in parallel to exclude bias. For mouse primary cell analyses, the genotype of mice was clearly marked on the housing cages and was well documented by the techniques. And in this case, the primary cells were allocated to different treatments randomly and treated in parallel to exclude bias.

Reporting for specific materials, systems and methods

We require information from authors about some types of materials, experimental systems and methods used in many studies. Here, indicate whether each material, system or method listed is relevant to your study. If you are not sure if a list item applies to your research, read the appropriate section before selecting a response.

Materials & experimental systems

n/a	Involved in the study
☐	☒ Antibodies
☒	☐ Eukaryotic cell lines
☒	☐ Palaeontology and archaeology
☐	☒ Animals and other organisms
☒	☐ Human research participants
☒	☐ Clinical data
☒	☐ Dual use research of concern

Methods

n/a	Involved in the study
☒	☐ ChIP-seq
☒	☐ Flow cytometry
☒	☐ MRI-based neuroimaging

Antibodies

Antibodies used	Western blot was performed with following antibodies that were obtained from Cell Signaling Technology: phospho-AMPKαT172 (#2531), AMPKα (#2532), GAPDH (#5174), HSP90 (#4874) and β-actin (#4970).
Validation	All antibodies were used in accordance to the manufacturer guidelines. And sizes of detected proteins were as expected. phospho-AMPKαT172 (#2531) were validated by the manufacturer and the following publication: Hardie, D.G. (2004) J Cell Sci 117, 5479-87. Carling, D. (2004) Trends Biochem Sci 29, 18-24. Hawley, S.A. et al. (1996) J Biol Chem 271, 27879-87. Lizcano, J.M. et al. (2004) EMBO J 23, 833-43. Shaw, R.J. et al. (2004) Proc Natl Acad Sci USA 101, 3329-35.

Woods, A. et al. (2003) J Biol Chem 278, 28434-42.
Warden, S.M. et al. (2001) Biochem J 354, 275-83.
Morales-Alamo, D. et al. (2013) J Appl Physiol 114, 566-77.
Fullerton, M.D. et al. (2013) Nat Med 19, 1649-54.

AMPKα (#2532) were validated by the manufacturer and the following publication:
Hardie, D.G. (2004) J Cell Sci 117, 5479-87.
Carling, D. (2004) Trends Biochem Sci 29, 18-24.
Hawley, S.A. et al. (1996) J Biol Chem 271, 27879-87.
Lizcano, J.M. et al. (2004) EMBO J 23, 833-43.
Shaw, R.J. et al. (2004) Proc Natl Acad Sci USA 101, 3329-35.
Woods, A. et al. (2003) J Biol Chem 278, 28434-42.
Warden, S.M. et al. (2001) Biochem J 354, 275-83.

GAPDH (#5174) were validated by the manufacturer and the following publication:
Barber, R.D. et al. (2005) Physiol. Genomics 21, 389-95.
Hara, M.R. and Snyder, S.H. Cell Mol Neurobiol (2006) 26, 527-38.
Zheng, L. et al. (2003) Cell 114, 255-66.
Bae, B.I. et al. (2006) Proc Natl Acad Sci USA 103, 3405-9.
Wang, Q. et al. (2005) FASEB J. 19, 869-71.
Kozako, T. et al. (2015) Sci Rep 5, 11345.

HSP90 (#4874) were validated by the manufacturer and the following publication:
Nollen, E.A. and Morimoto, R.I. (2002) J. Cell Sci. 115, 2809-2816.
Young, J.C. et al. (2003) Trends Biochem. Sci. 28, 541-547.
Pratt, W.B. and Toft, D.O. (2003) Exp. Biol. Med. 228, 111-133.
Hohfeld, J. et al. (2001) EMBO Rep. 2, 885-890.

β-actin (#4970) were validated by the manufacturer and the following publication:
Herman, I.M. (1993) Curr Opin Cell Biol 5, 48-55.
Perrin, B.J. and Ervasti, J.M. (2010) Cytoskeleton (Hoboken) 67, 630-4.
Condeelis, J. (2001) Trends Cell Biol 11, 288-93.
Lim, Y.P. et al. (2004) Clin Cancer Res 10, 3980-7.
Kayalar, C. et al. (1996) Proc Natl Acad Sci U S A 93, 2234-8.
Communal, C. et al. (2002) Proc Natl Acad Sci U S A 99, 6252-6.
Du, J. et al. (2004) J Clin Invest 113, 115-23.

And the use of β-actin (#4970) and phospho-AMPKαT172 (#2531) to detect C.elegans ACT-1 and phospho-AAK-2 has been validated by previous publications from independent research group:
C. elegans S6K Mutants Require a Creatine-Kinase-like Effector for Lifespan Extension. Cell Reports. 2016
Feedback regulation via AMPK and HIF-1 mediates ROS-dependent longevity in Caenorhabditis elegans. PNAS. 2014

Animals and other organisms

Policy information about studies involving animals; ARRIVE guidelines recommended for reporting animal research

Laboratory animals	Caenorhabditis elegans and mice were used in this study. For all C. elegans experiments, hermaphrodite worms were used. For the lifespan analyses, L4 stages were collected to start the experiments. For in vivo fluorescence/Calcium imaging analyses, Day1 to Day2 adult worms were used. Transgenic worms were generated following a standard microinjection protocol in the field. The genotypes of C. elegans strains used in this study were listed in the methods section. For mouse-related experiment, wild-type C57BL/6J mice (Stock no. 00664) were used and housed (24℃, 30% humidity) under 12 h light/12 h dark cycle (6 a.m.-6 p.m.) with a standard rodent chow diet (5L0D, PicoLab). mice (C57BL/6J, 6–8 weeks of age) of both genders were used for primary cells isolation and similar results were observed.
Wild animals	No wild animals were used in this study.
Field-collected samples	No field samples were collected for this study.
Ethics oversight	No ethnical approval is required to work with Caenorhabditis elegans. For mouse studies, all animal care and experimental protocol were reviewed and approved by the Institutional Animal Care and Use Committee at the University of Michigan.

Note that full information on the approval of the study protocol must also be provided in the manuscript.